

Harmony of Super Form Factors

A. Brandhuber^{a,b}, Ö. Gürdoğan^a, R. Mooney^a, G. Travaglini^{a,b} and G. Yang^{a1}

^a*Centre for Research in String Theory
School of Physics and Astronomy
Queen Mary University of London
Mile End Road, London, E1 4NS
United Kingdom*

^b*Kavli Institute for Theoretical Physics
University of California, Santa Barbara, CA 93106, USA*

Abstract

In this paper we continue our systematic study of form factors of half-BPS operators in $\mathcal{N}=4$ super Yang-Mills. In particular, we extend various on-shell techniques known for amplitudes to the case of form factors, including MHV rules, recursion relations, unitarity and dual MHV rules. As an application, we present the solution of the recursion relation for split-helicity form factors. We then consider form factors of the stress-tensor multiplet operator and of its chiral truncation, and write down supersymmetric Ward identities using chiral as well as non-chiral superspace formalisms. This allows us to obtain compact formulae for families of form factors, such as the maximally non-MHV case. Finally we generalise dual MHV rules in dual momentum space to form factors.

¹ {a.brandhuber,o.c.gurdogan,r.j.b.mooney,g.travaglini,g.yang}@qmul.ac.uk

Contents

1	Introduction	2
2	Tree-level methods	4
2.1	MHV diagrams	4
2.1.1	NMHV form factors	5
2.2	Recursion relations	6
2.2.1	Recursion relations for the split-helicity form factor	7
2.2.2	Solution for the split-helicity form factor	9
2.2.3	Examples	12
3	Supersymmetric form factors and Ward identities	15
3.1	Form factor of the chiral stress-tensor multiplet operator	15
3.2	Examples	19
3.2.1	Form factor of $\text{Tr}(\phi^{++}\phi^{++})$	19
3.2.2	Form factor of the on-shell Lagrangian	20
3.2.3	Why is the maximally non-MHV form factor so simple?	21
3.3	Form factor of the complete stress-tensor multiplet	22
4	Supersymmetric methods	24
4.1	Supersymmetric MHV rules	25
4.2	Supersymmetric recursion relations	26
4.3	Supersymmetric unitarity-based method	27
5	Dual MHV rules for form factors	27
5.1	Examples	29
5.2	Higher-loop diagrams	32
A	Vanishing of form factors at large z	35
A.1	Bosonic form factors	35

1 Introduction

Form factors are interesting physical observables which are situated at the interface between completely on-shell quantities such as scattering amplitudes and completely off-shell quantities like correlation functions. In a gauge theory one typically considers the overlap of a state created by a gauge-invariant operator $\mathcal{O}(x)$ with a multiparticle state $\langle 1 \cdots n |$ described by the particles' momenta p_1, \dots, p_n and other relevant quantum numbers such as the helicity, for massless particles. We will usually consider the Fourier transform of the form factor,

$$\int d^4x e^{-iqx} \langle 1 \cdots n | \mathcal{O}(x) | 0 \rangle = \delta^{(4)}(q - \sum_{i=1}^n p_i) \langle 1 \cdots n | \mathcal{O}(0) | 0 \rangle, \quad (1.1)$$

where the momentum delta function appears as a consequence of translational invariance of the theory, with $\mathcal{O}(x) = \exp(i\mathcal{P}x)\mathcal{O}(0)\exp(-i\mathcal{P}x)$.

Form factors appear in several interesting physical contexts. Some of the early applications include the amplitude for deep inelastic scattering, which is controlled by the matrix element $\langle X | J_{h,\mu}^{\text{e.m.}}(0) | p \rangle$ of the hadronic electromagnetic current $J_{h,\mu}^{\text{e.m.}}$ with an initial proton state p and a final hadronic state X , and the $e^+e^- \rightarrow X$ annihilation process, governed by the form factor $\langle X | J_{h,\mu}^{\text{e.m.}}(0) | 0 \rangle$. Furthermore, the universal structure of infrared divergences of amplitudes is controlled by the Sudakov form factor [1–7], with the coefficient of the leading infrared divergence being related to the cusp anomalous dimension [8] and the large-spin limit of twist-two operators [9]. Its universal, exponential form has inspired the all-loop conjecture for planar MHV amplitudes in $\mathcal{N} = 4$ super Yang Mills (SYM) [10]. Another interesting application of form factors is the operator product expansion of null polygonal Wilson loops proposed recently in [11].

Ultimately, one of the important goals and motivations for the study of form factors in $\mathcal{N} = 4$ SYM is that they interpolate between off-shell and on-shell quantities. For off-shell quantities such as two-point correlation functions, integrability has been developed into a powerful computational tool,¹ and it also plays an important role in the calculation of amplitudes [13, 14] and form factors [15, 16] at strong coupling.

¹For a recent review see [12] and references therein.

On the other hand, for amplitudes at weak coupling we have so far only glimpses of hidden integrable structures, and we hope that this interpolation will give us new insights on the role and uses of integrability in the context of amplitudes.

Form factors in maximally $\mathcal{N}=4$ super Yang-Mills at strong coupling were recently considered in [15, 16]. At weak coupling, they were first considered in [17], and in greater detail and generality in [18] and [19]. In particular, [18] considered form factors of the half-BPS scalar operator $\text{Tr}(\phi_{12}\phi_{12})$ in $\mathcal{N}=4$ SYM at tree level and one loop, where ϕ_{AB} are the six scalar fields in the theory, $A, B = 1, \dots, 4$, with $\phi_{AB} = -\phi_{BA}$, with external states containing two scalars and an arbitrary number of positive-helicity gluons. These MHV form factors were found to be remarkably simple. Specifically, at tree level they are expressed in terms of a holomorphic function of the spinor variables associated to the particle momenta which is a close cousin of the Parke-Taylor MHV scattering amplitude [20]. This simplicity was also found to persist at one loop, where the result for these MHV form factors is a remarkably simple expression which is very reminiscent of that for an n -point MHV amplitude at one loop.

In this paper we continue the systematic study initiated in [18]. The preceding discussion has already outlined two of the motivations for this study. Firstly, the attempt at connecting the on-shell world of scattering amplitudes (with a flurry of new techniques discovered over the past seven years) to that of off-shell observables in the theory, with integrability playing a prominent role in determining the quantum structure of some of these observables at strong and weak coupling. The second motivation is that form factors are expressed by simple formulae despite being partially off shell. As we shall see, certain form factors exhibit further unexpected simplicities, such as the maximally non-MHV form factors. More concretely, in this paper we pursue the following objectives.

In Section 2 we begin by extending to form factors some distinguished on-shell techniques used successfully over the past years to calculate amplitudes, such as MHV diagrams [21] and on-shell recursion relations [22, 23]. Some of these findings are not unexpected – for example, MHV rules are related to an MHV Lagrangian which is applicable also off shell [24], and recursion relations are based on factorisation, which is a general property not only of amplitudes but also of Green’s functions [25]. Notice that MHV diagrams are expected to work also in the presence of multiple operator insertions. As an application, we will explicitly solve the recursion relations for form factors where the external state is made of gluons in a split-helicity configuration. This parallels a corresponding explicit solution for amplitudes found in [26].

Section 3 — a central part of this paper — is devoted to supersymmetric form factors. We will find that harmonic superspace [27, 28] is a very convenient framework to formulate and study such objects. More precisely, we consider form factors where the operator inserted is the *chiral part* of the stress-tensor multiplet operator, which preserves half of the supersymmetries *off shell* [29, 30], while the state is described

using the supersymmetric formalism of Nair [31]. Using a chiral superspace formulation we write down supersymmetric Ward identities for these form factors, and show how they constrain their form. As a particular application of these techniques we derive the maximally non-MHV form factors which turn out to be surprisingly simple. Finally, we study form factors of the full stress-tensor multiplet operator for which we introduce a non-chiral superspace representation.

In Section 4 we briefly introduce supersymmetric MHV diagrams, supersymmetric recursion relations and unitarity for form factors. These generalisations are rather straightforward, so our presentation here is somewhat condensed.

Finally, in Section 5 we introduce dual MHV rules for form factors formulated directly in dual (super) momentum space by giving various examples at tree and one-loop level, and point out and explain certain subtleties encountered at higher loops. In this construction, a certain periodic kinematic configuration, emerging in the strong-coupling calculation of [15, 16], plays a central role, and we discuss similarities with (and differences from) the Wilson loop/amplitude duality [32–34].

The understanding of the large- z behaviour of form factors is crucial in formulating the recursion relation, and is analysed in detail in Appendix A. Finally, in Appendix B we provide a brief reminder of the dual MHV rules for amplitudes.

2 Tree-level methods

In this section we will develop and extend tree-level methods for form factors by generalising the corresponding methods for amplitudes, namely MHV diagrams [21] and on-shell recursions relations [22, 23].² We then proceed to obtain several new results including the NMHV and all split-helicity cases. We will not present the calculations with both methods for all examples but wish to stress here that we have made extensive checks to confirm that the results obtained with either method always agree. The supersymmetrisation of these methods will be considered in Section 4.

2.1 MHV diagrams

We start with a simple extension of the MHV diagram method [21] to form factors. We will test this here only in tree-level calculations, but the extension to loop level, following [36], is straightforward.

Specifically, we will be interested in calculating NMHV form factors of the simplest class of operators in $\mathcal{N} = 4$ SYM, namely the half-BPS operators $\text{Tr}(\phi_{12}\phi_{12})$. They

²For a recent review of tree-level methods in gauge theory and gravity, see [35].

take the form

$$\langle g^+(p_1) \cdots \phi_{12}(p_i) \cdots \phi_{12}(p_j) \cdots g^+(p_{n-1}) g^-(p_n) | \text{Tr}(\phi_{12}\phi_{12})(x) | 0 \rangle , \quad (2.1)$$

where all but one of the gluons have positive helicity. The strategy of the calculation is very simple – we need to augment the set of usual MHV vertices for amplitudes by including a new family of MHV vertices, obtained by continuing off shell the tree-level MHV form factors of the half-BPS operators. The expressions for these quantities were derived in [18], and are given by

$$\begin{aligned} & \int d^4x e^{-iqx} \langle g^+(p_1) \cdots \phi_{12}(p_i) \cdots \phi_{12}(p_j) \cdots g^+(p_n) | \text{Tr}(\phi_{12}\phi_{12})(x) | 0 \rangle \\ &= g^{n-2} (2\pi)^4 \delta^{(4)} \left(\sum_{k=1}^n \lambda_k \tilde{\lambda}_k - q \right) F_{\text{MHV}} , \end{aligned} \quad (2.2)$$

where

$$F_{\text{MHV}} = \frac{\langle ij \rangle^2}{\langle 12 \rangle \cdots \langle n1 \rangle} . \quad (2.3)$$

Here $p_m := \lambda_m \tilde{\lambda}_m$ are on-shell momenta of the external particles, and $q := \sum_{m=1}^n p_m$ is the momentum carried by the operator insertion. It was observed in [18] that, since (2.3) is a holomorphic function of the spinor variables, the MHV form factors are localised on a complex line in twistor space, similarly to the MHV amplitudes [37].

Using localisation as an inspiration, we propose to use an appropriate off-shell continuation of (2.3) as a new vertex to construct the perturbative expansion of non-MHV form factors of the operator $\text{Tr}(\phi_{12}\phi_{12})$. The off-shell continuation is the standard one introduced in [21]. The momentum L of an internal, off-shell particle is decomposed as $L = l + z\xi$, where $l = \lambda_L \tilde{\lambda}_L$ is an on-shell momentum and ξ an arbitrary reference null momentum. The off-shell continuation of [21] consists then in using the spinor λ_L as the spinor variable associated with the internal leg of momentum L , where

$$\lambda_{L,\alpha} = \frac{L_{\alpha\dot{\alpha}} \tilde{\xi}^{\dot{\alpha}}}{[\tilde{\lambda}_L, \tilde{\xi}]} . \quad (2.4)$$

The denominator in the right-hand side of (2.4) will be irrelevant for our applications since each MHV diagram is invariant under rescalings of the internal spinor variables. Hence, we will discard it and simply replace $\lambda_{L,\alpha} \rightarrow L_{\alpha\dot{\alpha}} \tilde{\xi}^{\dot{\alpha}}$.

2.1.1 NMHV form factors

Using the MHV rules outlined in the previous section, we now present an example of derivation of an NMHV form factor. Specifically, the form factor we consider is

$$F_{\text{NMHV}}(1_{\phi_{12}}, 2_{\phi_{12}}, 3_{g^-}, 4_{g^+}) := \langle \phi_{12}(p_1) \phi_{12}(p_2) g^-(p_3) g^+(p_4) | \text{Tr}(\phi_{12}\phi_{12})(0) | 0 \rangle . \quad (2.5)$$

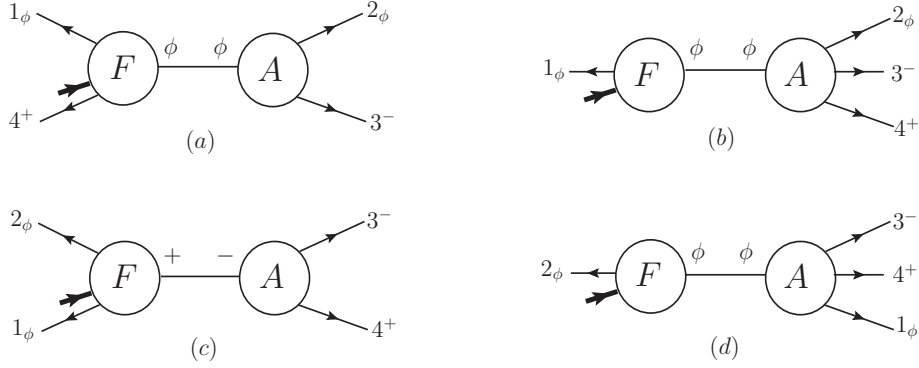


Figure 1: *The four MHV diagrams contributing to the NMHV form factor (2.5).*

There are four MHV diagrams contributing to (2.5), depicted in Figure 1. A short calculation shows that these are given by the following expressions:

$$\begin{aligned}
\text{Diagram (a)} &= \frac{[2\xi]}{[\xi 3]} \frac{1}{[32]\langle 41\rangle} \frac{\langle 1|q-p_4|\xi]}{\langle 4|q-p_1|\xi]} , \\
\text{Diagram (b)} &= \frac{\langle 23\rangle}{\langle 34\rangle s_{234}} \frac{\langle 3|p_2+p_4|\xi]^2}{\langle 2|p_3+p_4|\xi]\langle 4|p_2+p_3|\xi]} , \\
\text{Diagram (c)} &= \frac{\langle 12\rangle [\xi 4]^3}{[43] [3\xi]} \frac{1}{\langle 2|p_3+p_4|\xi]\langle 1|p_3+p_4|\xi]} , \\
\text{Diagram (d)} &= \frac{1}{s_{341}} \frac{\langle 13\rangle^2}{\langle 34\rangle\langle 41\rangle} \frac{\langle 3|p_4+p_1|\xi]}{\langle 1|p_3+p_4|\xi]} . \tag{2.6}
\end{aligned}$$

We have checked that the sum of all MHV diagrams is independent of the choice of the reference spinor $\tilde{\xi}$. A particularly convenient choice of $\tilde{\xi}$ is $\tilde{\xi} = \tilde{\lambda}_4$, in which case we get

$$\begin{aligned}
F_{\text{NMHV}}(1_{\phi_{12}}, 2_{\phi_{12}}, 3_{g^-}, 4_{g^+}) &= \frac{[24]}{[34]} \frac{1}{\langle 4|p_2+p_3|4]} \left[\frac{\langle 1|q|4]}{[23]\langle 41\rangle} + \frac{[24]\langle 23\rangle^2}{\langle 34\rangle} \frac{1}{s_{234}} \right] \\
&+ \frac{\langle 13\rangle^2 [14]}{\langle 41\rangle\langle 34\rangle[43]} \frac{1}{s_{341}} . \tag{2.7}
\end{aligned}$$

It is straightforward to apply this procedure to more general form factors but for brevity we will not present them here. However, we mention that all results derived in the next subsection using recursion relations have been compared with formulae obtained from MHV diagrams finding a perfect match in all cases.

2.2 Recursion relations

In this subsection we study the application of recursion relations to the derivation of tree-level form factors. As a warm-up we will re-derive the NMHV form factor in

(2.5) finding agreement with (2.7), and then move on to consider more general cases including split-helicity configurations. Since form factors contain a single operator insertion, it is clear that every recursive diagram will contain one amplitude and one form factor as the factorisation properties used in the case of tree-level recursions for amplitudes also apply to tree-level form factors. This is the only modification to the on-shell recursion relations of [22]. In Appendix A we discuss the behaviour of form factors under large complex deformations, and confirm the validity of the calculations below, i.e. we show that under the shifts used the form factors vanish as $z \rightarrow \infty$.

Let us begin by re-deriving the NMHV form factor (2.5). We will use a $[34]$ shift, namely

$$\hat{\tilde{\lambda}}_3 := \tilde{\lambda}_3 + z\tilde{\lambda}_4, \quad \hat{\lambda}_4 := \lambda_4 - z\lambda_3. \quad (2.8)$$

There are two recursive diagrams, depicted in Figure 2 below. A short calculation shows that

$$\begin{aligned} \text{Diagram (a)} &= \frac{[24]^2}{[23][34]} \frac{1}{s_{234}} \frac{\langle 1|q|4 \rangle}{\langle 1|q|2 \rangle}, \\ \text{Diagram (b)} &= \frac{\langle 13 \rangle^2}{\langle 34 \rangle \langle 41 \rangle} \frac{1}{s_{341}} \frac{\langle 3|q|2 \rangle}{\langle 1|q|2 \rangle}, \end{aligned} \quad (2.9)$$

so that

$$F_{\text{NMHV}}(1_{\phi_{12}}, 2_{\phi_{12}}, 3_{g^-}, 4_{g^+}) = \frac{1}{\langle 1|q|2 \rangle} \left[\frac{[24]^2}{[23][34]} \frac{1}{s_{234}} \langle 1|q|4 \rangle + \frac{\langle 13 \rangle^2}{\langle 34 \rangle \langle 41 \rangle} \frac{1}{s_{341}} \langle 3|q|2 \rangle \right]. \quad (2.10)$$

It is interesting to note that the $1/\langle 1|q|2 \rangle$ pole is in fact spurious. This can be shown by using the identities

$$\begin{aligned} \langle 1|q p_4|3 \rangle + \langle 1|q p_2|3 \rangle &= \langle 13 \rangle s_{234}, \\ [4|p_3 q|2 \rangle + [4|p_1 q|2 \rangle &= [42] s_{341}, \end{aligned} \quad (2.11)$$

which allow to recast the form factor in the alternative form

$$F_{\text{NMHV}}(1_{\phi_{12}}, 2_{\phi_{12}}, 3_{g^-}, 4_{g^+}) = \frac{1}{s_{34} [23] \langle 41 \rangle} \left[\frac{\langle 14 \rangle \langle 23 \rangle [24]^2}{s_{234}} + \frac{[41][32] \langle 13 \rangle^2}{s_{341}} + [24] \langle 13 \rangle \right]. \quad (2.12)$$

We have checked that our result (2.7) for the form factor derived using MHV diagrams, and (2.12), obtained using recursion relations, are in agreement.

2.2.1 Recursion relations for the split-helicity form factor

In the previous section we found that the BCF recursion relation for the NMHV form factor with a $[3, 4]$ shift has just two diagrams. This property in fact holds for all form factors of the form $F_{\phi^2; q-2, n-q}(1_\phi, 2_\phi, 3^-, \dots, q^-, (q+1)^+, \dots, n^+)$, which we call

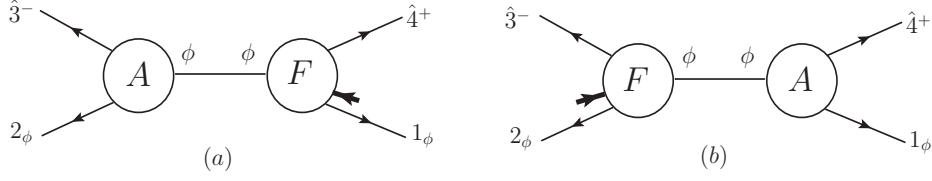


Figure 2: *The two recursive diagrams contributing to the NMHV form factor (2.5).*

henceforth *split-helicity*. As we will show shortly, performing a $[q, q+1]$ shift leads to a general, closed-form solution of the BCFW recursion relations for this special class of form factors. Note that all split-helicity gluon scattering amplitudes were computed in [26] – we construct here a similar solution for form factors.

Each recursive diagram with a $[q, q+1]$ shift contains a three-point amplitude and an $(n-1)$ -point form factor. We can neatly combine the three-point amplitude and the propagator in a prefactor to write³

$$F_{q-2, n-q} = \frac{[q-1q+1]}{[q-1q][qq+1]} F_{q-3, n-q}(1_\phi, 2_\phi, 3^-, \dots, \widehat{q-1}^-, \widehat{q+1}^+, \dots, n^+) \quad (2.13)$$

$$+ \frac{\langle qq+2 \rangle}{\langle qq+1 \rangle \langle q+1q+2 \rangle} F_{q-2, n-q-1}(1_\phi, 2_\phi, 3^-, \dots, \hat{q}^-, \widehat{q+2}^+, \dots, n^+),$$

where the shifted spinors of the external momenta that appear in the lower-point form factors are

$$\lambda_{\widehat{q+1}} = \frac{[q-1|P_{q,q+1}}{[q-1q+1]}, \quad (2.14a)$$

$$\tilde{\lambda}_{\hat{q}} = \frac{P_{q,q+2}|q+2\rangle}{\langle qq+2\rangle}, \quad (2.14b)$$

with $P_{a,b} = p_a + \dots + p_b$. Furthermore, the shifted spinors associated with internal legs are relabelled as

$$\lambda_{\hat{P}_{q-1q}}(z = z_{q-1q}) \rightarrow \lambda_{\widehat{q-1}} = \frac{P_{q,q+1}|q+1\rangle}{[q-1q+1]}, \quad (2.15a)$$

$$\tilde{\lambda}_{\hat{P}_{q+1q+2}}(z = z_{q+1q+2}) \rightarrow \tilde{\lambda}_{\widehat{q+2}} = \frac{\langle q|P_{q,q+2}}{\langle qq+2\rangle}, \quad (2.15b)$$

so that the notation remains compatible with subsequent recursions. Crucially, all lower-point form factors appearing in (2.13) are of split-helicity form, so that the split helicity form factors are closed under recursions. Once we have reduced the

³For the rest of this section we will always assume that the operator $\mathcal{O} = \text{Tr}(\phi_{12}\phi_{12})$ is inserted and will not mention it explicitly. Although the solution is presented for this particular insertion, the construction can be generalised to form factors involving other operators.

form factor to expressions that involve only MHV and $\overline{\text{MHV}}$ terms, we can insert the shifted momenta.

It is useful to illustrate the structure of the recursion relations for split-helicity form factors using a square lattice as in Figure 3. Consider for example the form factor $F_{2,2}$. In this case, the first iteration using equation (2.13) relates $F_{2,2}$ to the form factors $F_{2,1}$ and $F_{1,2}$, which however are neither MHV nor $\overline{\text{MHV}}$. The next iteration leads to an expression involving one $F_{2,0}$, two $F_{1,1}$'s and one $F_{0,2}$ evaluated at some shifted momenta. A final iteration would then allow us to express the answer in terms of MHV and $\overline{\text{MHV}}$ form factors alone, or even to reduce everything down to $F_{0,0}$. It is also easy to see that this pattern generalises to arbitrary split-helicity form factors and that each term generated by subsequent recursions corresponds to a unique path between the form factor and the MHV or $\overline{\text{MHV}}$ edges of the lattice, as illustrated in Figure 3.

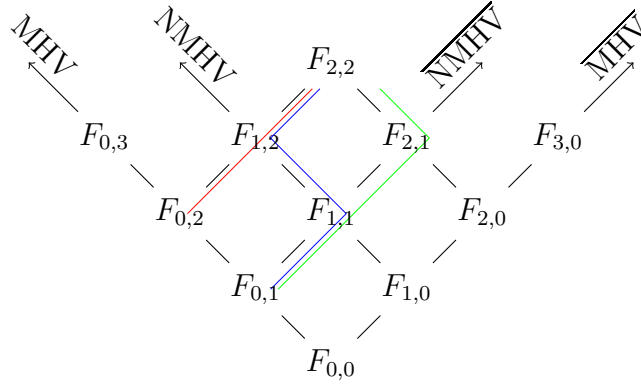


Figure 3: *The iterative structure of split-helicity form factors illustrated by a square lattice. The three coloured paths ending on the MHV line are in one-to-one correspondence with terms that appear in the iterated recursion of $F_{2,2}$. Similarly there will be three paths (terms) that end on the $\overline{\text{MHV}}$ line.*

In principle, all we need to do to compute a split-helicity form factor is to collect all prefactors picked up at each step of the recursion process and follow the iterated momentum shifts along a particular path on the lattice.

2.2.2 Solution for the split-helicity form factor

A very efficient way to organise the recursion is in terms of *zig-zag diagrams*, like those introduced in [26] for split-helicity gluon amplitudes. It is natural to split the terms of the solution into those corresponding to paths ending on the MHV or $\overline{\text{MHV}}$ lines, respectively.

Zig-zag diagrams that correspond to recursion terms with an MHV form factor will be denoted as MHV zig-zags and the ones with an $\overline{\text{MHV}}$ form factor as $\overline{\text{MHV}}$

zig-zags. Note that we have therefore two types of diagrams, in contrast to the case of amplitudes in [26]. One can make this separation also for amplitudes as it only means that we terminate the iterated recursion once we reach an $\overline{\text{MHV}}$ term, instead of recursing it further down to $F_{0,0}$ (or $A_{2,2}$ for the case of amplitudes). In the path picture of the previous section, this separation corresponds to the fact that there is a unique path between any $\overline{\text{MHV}}$ form factor and $F_{0,0}$, hence one can replace that part of the recursion directly with an $\overline{\text{MHV}}$ form factor. Because the MHV zig-zags defined below are not compatible with two point objects such as $F_{0,0}$ we chose to use this formalism with two types of diagrams. This has the added advantage that it makes the parity symmetry of $F_{q-2,q-2}$ form factors manifest.

The MHV zig-zags are parameterised with $2k + 1$ labels

$$2 \leq a_1 < \dots < a_k < q - 1 \quad \text{and} \quad n \geq b_1 > \dots > b_{k+1} > q, \quad k \geq 0,$$

representing expressions in the following manner

$$= \frac{N_1 N_2 N_3}{D_1 D_2 D_3} \quad (2.16)$$

while the $\overline{\text{MHV}}$ zig-zags are parametrised with $2k + 1$ labels

$$2 \leq \bar{b}_1 < \dots < \bar{b}_{k+1} < q \quad \text{and} \quad n \geq \bar{a}_1 > \dots > \bar{a}_k > q + 1, \quad k \geq 0,$$

representing expressions, similarly shown below

$$= \frac{\bar{N}_1 \bar{N}_2 \bar{N}_3}{\bar{D}_1 \bar{D}_2 \bar{D}_3} \quad (2.17)$$

where $N_{1,2,3}$ and $D_{1,2,3}$ are defined as

$$\begin{aligned}
N_1 &= \langle 1 | P_{2,b_1} P_{a_1+1,b_1} P_{a_1+1,b_2} P_{a_2+1,b_2} \cdots P_{q,b_{k+1}} | q \rangle \\
&\quad \times [2 | P_{a_1+1,b_1} P_{a_1+1,b_2} P_{a_2+1,b_2} \cdots P_{q,b_{k+1}} | q \rangle^2 \\
N_2 &= \langle b_1 + 1 | b_1 \rangle \langle b_2 + 1 | b_2 \rangle \cdots \langle b_{k+1} + 1 | b_{k+1} \rangle \\
N_3 &= [a_1 a_1 + 1] \cdots [a_k a_k + 1] \\
D_1 &= P_{2,b_1}^2 P_{a_1+1,b_1}^2 P_{a_1+1,b_2}^2 P_{a_2+1,b_2}^2 \cdots P_{q,b_{k+1}}^2 \\
D_2 &= Z_{q,1} \bar{Z}_{2,q-1} \\
D_3 &= [2 | P_{2,b_1} | b_1 + 1 \rangle \langle b_1 | P_{a_1+1,b_1} | a_1 \rangle [a_1 + 1 | P_{a_1+1,b_2} | b_2 + 1 \rangle \cdots \langle b_{k+1} | P_{q,b_{k+1}} | q - 1 \rangle] \\
&\hspace{15em} (2.18a)
\end{aligned}$$

$$\begin{aligned}
\bar{N}_1 &= [q + 1 | P_{\bar{b}_{k+1}+1,q+1}, \dots, P_{\bar{b}_2+1,\bar{a}_2}, P_{\bar{b}_2+1,\bar{a}_1}, P_{\bar{b}_1+1,\bar{a}_1} | 1 \rangle^2 \\
&\quad \times [q + 1 | P_{\bar{b}_{k+1}+1,q+1}, \dots, P_{\bar{b}_2+1,\bar{a}_2}, P_{\bar{b}_2+1,\bar{a}_1}, P_{\bar{b}_1+1,\bar{a}_1} P_{\bar{b}_1+1,1} | 2 \rangle] \\
\bar{N}_2 &= [\bar{b}_1 \bar{b}_1 + 1] \cdots [\bar{b}_{k+1} \bar{b}_{k+1} + 1] \\
\bar{N}_3 &= \langle \bar{a}_1 + 1 | \bar{a}_1 \rangle \cdots \langle \bar{a}_k + 1 | \bar{a}_k \rangle \\
\bar{D}_1 &= P_{\bar{b}_1+1,1}^2 P_{\bar{b}_1+1,\bar{a}_1}^2 P_{\bar{b}_2+1,\bar{a}_1}^2 \cdots P_{\bar{b}_k+1,q+1}^2 \\
\bar{D}_2 &= \bar{Z}_{2,q+1} Z_{q+2,1} \\
\bar{D}_3 &= \langle 1 | P_{\bar{b}_1+1,1} | \bar{b}_1 \rangle [\bar{b}_1 + 1 | P_{\bar{b}_1+1,\bar{a}_1} | \bar{a}_1 + 1 \rangle \langle \bar{a}_1 | P_{\bar{b}_2+1,\bar{a}_1} | \bar{b}_2 \rangle \cdots [\bar{b}_k + 1 | P_{\bar{b}_k+1,q+1} | q + 2 \rangle], \\
&\hspace{15em} (2.18b)
\end{aligned}$$

with

$$Z_{i,j} = \langle i | i + 1 \rangle \cdots \langle j - 1 | j \rangle, \quad \bar{Z}_{i,j} = [i | i + 1] \cdots [j - 1 | j]. \quad (2.18c)$$

The split-helicity form factor is then the sum of all recursion terms, or equivalently the sum of all possible MHV and $\overline{\text{MHV}}$ zig-zags, which is equal to

$$F_{q-2,n-q-2} = \sum_{\{a_i, b_i\}} \frac{N_1 N_2 N_3}{D_1 D_2 D_3} + \sum_{\{\bar{a}_i, \bar{b}_i\}} \frac{\bar{N}_1 \bar{N}_2 \bar{N}_3}{\bar{D}_1 \bar{D}_2 \bar{D}_3}. \quad (2.19)$$

Notice that for the form factors with equal number of negative and positive helicity gluons, the $\overline{\text{MHV}}$ zig-zags can be obtained from the MHV ones by changing $(2, 3, \dots, q) \rightarrow (1, n, \dots, q + 1)$ and $\langle ij \rangle \rightarrow [ji]$.

Let us now explain the precise relation between the zig-zag diagrams and the paths on the split-helicity form factor lattice. Let a path with r_1 steps to the right, l_1 steps to the left followed by r_2 steps to the right etc. be represented by

$$R^{r_k} \cdots R^{r_2} L^{l_1} R^{r_1}. \quad (2.20)$$

Then an MHV zig-zag labelled by $\{a_i, b_i\}$ corresponds to the path:

$$L^{a_1-1} R^{b_1-b_2} \cdots L^{a_k-a_{k-1}} R^{b_k-b_{k+1}} L^{q-1-a_k} R^{b_k-(q+1)},$$

while an $\overline{\text{MHV}}$ zig-zag labelled by $\{\bar{a}_i, \bar{b}_i\}$ corresponds to the path:

$$R^{\bar{a}_1+1} L^{\bar{b}_2-\bar{b}_1} \dots R^{\bar{a}_k-\bar{a}_{k-1}} L^{\bar{b}_{k+1}-\bar{b}_k} R^{\bar{a}_k-q-1} L^{q-\bar{b}_{k+1}-1}.$$

Note that if there are no a_i indices in the MHV zig-zag diagram we set $a_1 = 1$; and if there are no \bar{a}_i in the $\overline{\text{MHV}}$ zig-zag diagram we set $\bar{a}_1 = n$. All powers in the above formulae are modulo n .

2.2.3 Examples

Here we present some examples to show that the solution (2.19) reproduces the correct expressions.

MHV case

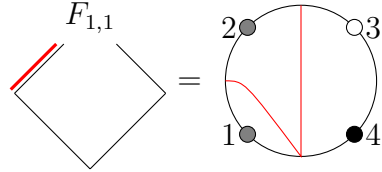
The zig-zag diagrams collapse onto a point between 1 and 2 as there are neither b_i nor \bar{a}_i . Hence, the only contributions are $N_1 = \langle 12 \rangle$ and $D_2 = F_{2,1}$ and

$$F_{1,n-3}(1_\phi, 2_\phi, 3^+, \dots, n^+) = \frac{\langle 12 \rangle}{\langle 23 \rangle \langle 34 \rangle \dots \langle n1 \rangle}, \quad (2.21)$$

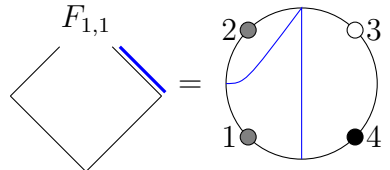
as required. The situation for MHV amplitudes is similar [26]. An equivalent calculation for the $\overline{\text{MHV}}$ zig-zag gives the $\overline{\text{MHV}}$ form factor.

NMHV case

At four points, there is exactly one MHV and one $\overline{\text{MHV}}$ zig-zag, representing one move to the left and one move to the right. Comparing with equations (2.16) and (2.17) one can read off $b_1 = 4$ for the MHV zig-zag and $\bar{b}_1 = 2$ for the $\overline{\text{MHV}}$ zig-zag.



$$F_{1,1} = \text{[Diagram]} = \frac{[24]^2}{[32][43]} \frac{\langle 1|q|4 \rangle}{\langle 1|q|2 \rangle} \frac{1}{s_{234}} \quad (2.22)$$



$$F_{1,1} = \text{[Diagram]} = \frac{\langle 13 \rangle^2}{\langle 34 \rangle \langle 41 \rangle} \frac{\langle 3|q|2 \rangle}{\langle 1|q|2 \rangle} \frac{1}{s_{341}} \quad (2.23)$$

This result is in agreement with the previous section.

In general, for the NMHV form factors, there is one $\overline{\text{MHV}}$ zig-zag corresponding to the path which proceeds along the NMHV line until it reaches the $\overline{\text{MHV}}$ edge of the lattice, and $n - 3$ MHV zig-zags where the path shifts onto the MHV edge before it arrives at the $\overline{\text{MHV}}$ edge. The MHV paths and the corresponding zig-zags are shown in Figure 4.

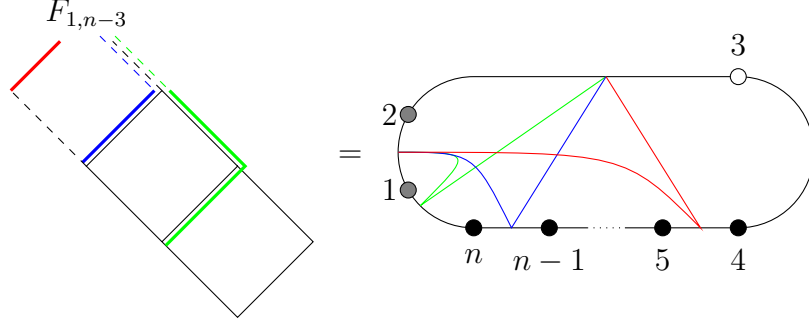


Figure 4: *Correspondence of lattice paths and MHV zig-zags for NMHV form factors.*

An N^2 MHV example

As it can be seen from the lattice in Figure 3, there are three MHV and three $\overline{\text{MHV}}$ terms in the recursion of the six-point split-helicity form factor. These are listed below, where the subscripts encode the shape of the path as described earlier. For example, F_{RLL} is the term which corresponds to the path that starts with a step to right and terminates at the MHV edge with two steps to the left. The MHV terms are:

- $b_1 = 5$, no a :

$$F_{LL} = \text{Diagram} = -\frac{[25]^2}{[23][34][45]\langle 61 \rangle} \frac{1}{P_{2,5}^2} \frac{[5|P_{2,4}|1\rangle}{[2|P_{2,5}|6]} \quad (2.24a)$$

- $b_1 = 6$, no a :

$$F_{RLL} = \text{Diagram} = \frac{1}{\langle 45 \rangle \langle 56 \rangle [23]} \frac{1}{P_{2,6}^2 P_{4,6}^2} \frac{\langle 1|P_{2,6}P_{4,6}|4\rangle [2|P_{4,6}|4\rangle^2}{[2|P_{2,6}|1\rangle \langle 6|P_{4,6}|3\rangle} \quad (2.24b)$$

- $b_1 = 6$, $b_2 = 5$, $a_1 = 2$:

$$F_{LRL} = \text{Diagram} = \frac{1}{[34][45]} \frac{1}{P_{2,6}^2 P_{3,6}^2 P_{3,5}^2} \frac{\langle 1|P_{2,6}P_{3,6}P_{3,5}|5\rangle [2|P_{3,6}P_{3,5}|5]^2}{[2|P_{2,6}|1\rangle \langle 6|P_{3,6}|2\rangle [3|P_{3,5}|6\rangle]} \quad (2.24c)$$

The $\overline{\text{MHV}}$ terms are:

- $\bar{b}_1 = 3$, no \bar{a}

$$F_{RR} = \text{Diagram} = \frac{\langle 14 \rangle^2}{\langle 45 \rangle \langle 56 \rangle \langle 61 \rangle [23]} \frac{1}{P_{4,1}^2} \frac{\langle 4|P_{4,1}|2\rangle}{\langle 1|P_{4,1}|3\rangle} \quad (2.25a)$$

- $\bar{b}_1 = 2$, no \bar{a}

$$F_{LRR} = \text{Diagram} = \frac{1}{[34][45]\langle 61 \rangle} \frac{1}{P_{3,5}^2 P_{3,1}^2} \frac{\langle 1|P_{3,5}|5\rangle^2 [5|P_{3,5}P_{3,1}|2\rangle}{\langle 1|P_{3,1}|2\rangle [3|P_{3,5}|6\rangle]} \quad (2.25b)$$

- $\bar{b}_1 = 2$, $b_2 = 3$, $\bar{a}_1 = 6$

$$F_{RLR} = \text{Diagram} = \frac{1}{\langle 45 \rangle \langle 56 \rangle} \frac{1}{P_{3,1}^2 P_{3,6}^2 P_{4,6}^2} \frac{\langle 4|P_{4,6}P_{3,1}|1\rangle^2 \langle 5|P_{4,6}P_{3,6}P_{3,1}|2\rangle}{\langle 1|P_{3,1}|2\rangle [3|P_{3,6}|1\rangle \langle 6|P_{4,6}|3\rangle [4|P_{4,6}|6\rangle]} \quad (2.25c)$$

We have checked this result against an MHV diagram calculation and both methods yield the same result.

3 Supersymmetric form factors and Ward identities

The purpose of this section is to write down supersymmetric Ward identities for certain appropriately defined form factors of supersymmetric operators. By solving these Ward identities, we will learn about the structure of these form factors.

To begin, we recall the familiar fact that in $\mathcal{N} = 4$ SYM one can efficiently package all scattering amplitudes with fixed total helicity and fixed number of particles n into a superamplitude [31], thereby making manifest some of the supersymmetries of the theory. This object depends on auxiliary fermionic variables $\eta_{i,A}$, one for each particle $i = 1, \dots, n$, with A an anti-fundamental $SU(4)$ index. The superamplitude can be Taylor-expanded in the η variables, with a specific correspondence between powers of η and particular external states. This correspondence can be read off from the Nair super-wavefunction [31], which encodes all the annihilation operators of the physical states,

$$\Phi(p, \eta) := g^+(p) + \eta_A \lambda^A(p) + \frac{\eta_A \eta_B}{2!} \phi^{AB}(p) + \epsilon^{ABCD} \frac{\eta_A \eta_B \eta_C}{3!} \bar{\lambda}_D(p) + \eta_1 \eta_2 \eta_3 \eta_4 g^-(p), \quad (3.1)$$

where $(g^+(p), \dots, g^-(p))$ are the annihilation operators of the corresponding states. In order to select a state with a particular helicity h_i , we need to expand the superamplitude and pick the term with $2 - 2h_i$ powers of η_i .

This familiar framework becomes richer for form factors. Indeed, one can consider form factors of bosonic operators – such as $\text{Tr}(\phi_{AB}\phi_{AB})$ – with an external supersymmetric state described using the Nair approach, but one can also supersymmetrise the operator itself, as we shall see in the next section.

A comment on notation – we denote a form factor as $\langle 0 | \Phi(1) \dots \Phi(n) \mathcal{O} | 0 \rangle$ or equivalently $\langle 1 \dots n | \mathcal{O} | 0 \rangle$, where $|i\rangle := \Phi^\dagger(i) | 0 \rangle$ is a Nair superstate, which satisfies

$$\langle i | P = \langle i | p_i, \quad \langle i | Q = \langle i | \lambda_i \eta_i, \quad \langle i | \bar{Q} = \langle i | \frac{\partial}{\partial \eta_i} \tilde{\lambda}_i, \quad (3.2)$$

where the derivative in the last equation acts on the state on its left. We also adopt the notation $\langle 1 \dots n | := \langle 0 | \Phi(1) \dots \Phi(n)$.

3.1 Form factor of the chiral stress-tensor multiplet operator

We now consider the form factor of the chiral supersymmetric operator⁴ $\mathcal{T}(x, \theta^+)$ considered recently in [29, 30]. This operator is the chiral part of the stress-tensor

⁴ A quick reminder of harmonic superspace [27, 28] conventions, following closely [29, 30]. We introduce the harmonic projections of the θ_α^A and $\bar{\theta}_{\dot{\alpha}}^A$ superspace coordinates and of the supersymmetry charges Q_A^α , $\bar{Q}_{\dot{\alpha}}^A$, as $\theta_\alpha^{+a} := \theta_\alpha^A u_A^{+a}$, $\bar{\theta}_{-a}^{\dot{\alpha}} := \bar{\theta}_{\dot{\alpha}}^A \bar{u}_{-a}^A$, and $Q_{\pm a}^\alpha := \bar{u}_{\pm a}^A Q_A^\alpha$, $\bar{Q}_{\dot{\alpha}}^{+a} := u_A^{+a} \bar{Q}_{\dot{\alpha}}^A$ with the harmonic $SU(4)$ u and \bar{u} normalised as in Section 3 of [29].

multiplet operator, $\mathcal{T}(x, \theta^+) := \mathcal{T}(x, \theta^+, \bar{\theta}_- = 0, u)$ and we report here its expression from [29] for convenience,

$$\begin{aligned} \mathcal{T}(x, \theta^+) &= \text{Tr}(\phi^{++}\phi^{++}) + i2\sqrt{2}\theta_\alpha^{+a}\text{Tr}(\lambda_a^{+\alpha}\phi^{++}) \\ &+ \theta_\alpha^{+a}\epsilon_{ab}\theta_\beta^{+b}\text{Tr}\left(\lambda^{+c(\alpha}\lambda_c^{+\beta)} - i\sqrt{2}F^{\alpha\beta}\phi^{++}\right) \\ &- \theta_\alpha^{+a}\epsilon^{\alpha\beta}\theta_\beta^b\text{Tr}\left(\lambda_{(a}^{+\gamma}\lambda_{b)\gamma}^+ - g\sqrt{2}[\phi_a^{+C}, \bar{\phi}_{C+b}] \phi^{++}\right) \\ &- \frac{4}{3}(\theta^+)^3_\alpha \text{Tr}\left(F_\beta^\alpha \lambda_a^{+\beta} + ig[\phi_a^{+B}, \bar{\phi}_{BC}]\lambda^{C\alpha}\right) + \frac{1}{3}(\theta^+)^4 \mathcal{L} . \end{aligned} \quad (3.3)$$

Notice that the $(\theta^+)^0$ component is nothing but the scalar operator $\text{Tr}(\phi^{++}\phi^{++})$, whereas the $(\theta^+)^4$ component is the on-shell Lagrangian.

Next we describe how to use supersymmetric Ward identities in order to constrain form factors, slightly extending the usual procedure for amplitudes. Ward identities associated with a certain symmetry generator s which leaves the vacuum invariant are obtained in a standard way [38–41] by expanding the identity

$$0 = \langle 0 | [s, \Phi(1) \cdots \Phi(n) \mathcal{O}] | 0 \rangle , \quad (3.4)$$

or

$$0 = \langle 0 | \Phi(1) \cdots \Phi(n) [s, \mathcal{O}] | 0 \rangle + \sum_{i=1}^n \langle 0 | \Phi(1) \cdots [s, \Phi(i)] \cdots \Phi(n) \mathcal{O} | 0 \rangle . \quad (3.5)$$

For instance, by considering s to be the momentum generator \mathcal{P} and using $[\mathcal{P}_\mu, \mathcal{O}(x)] = -i\partial_\mu \mathcal{O}(x)$ as well as the first equation of (3.2), we obtain

$$-i \langle 0 | \Phi(1) \cdots \Phi(n) \partial_\mu \mathcal{O}(x) | 0 \rangle + \left(\sum_{i=1}^n p_i \right) \langle 0 | \Phi(1) \cdots \Phi(n) \mathcal{O}(x) | 0 \rangle = 0 . \quad (3.6)$$

Fourier transforming x to q and integrating by parts one obtains

$$(q - \sum_{i=1}^n p_i) F(q; 1, \dots, n) = 0 , \quad (3.7)$$

where

$$F(q; 1, \dots, n) := \int d^4x e^{-iqx} \langle 1 \cdots n | \mathcal{O}(x) | 0 \rangle . \quad (3.8)$$

From this it follows that

$$F(q; 1, \dots, n) = C \cdot \delta^{(4)}(q - \sum_{i=1}^n p_i) . \quad (3.9)$$

C can be fixed by further integrating both sides of (3.9) with a d^4q measure and using (3.8), which leads to $C = \langle 0 | \Phi(1) \cdots \Phi(n) \mathcal{O}(0) | 0 \rangle = \langle 1 \cdots n | \mathcal{O}(0) | 0 \rangle$.

Similarly, we now consider Ward identities for the harmonic projections $Q_{\pm a}^\alpha$, $a = 1, 2$, of the Q -supersymmetry generators. We obtain

$$0 = \langle 0 | \Phi(1) \cdots \Phi(n) [Q_\pm, \mathcal{T}(x, \theta^+)] | 0 \rangle + \sum_{i=1}^n \langle 0 | \Phi(1) \cdots [Q_\pm, \Phi(i)] \cdots \Phi(n) \mathcal{T}(x, \theta^+) | 0 \rangle . \quad (3.10)$$

We now have to discuss how supersymmetry acts on the chiral part of $\mathcal{T}(x, \theta^+)$ as well as on the states.

In general the supersymmetry algebra closes only up to gauge transformations and equations of motion,⁵ however we consider here gauge-invariant operators such as \mathcal{T} which, furthermore, are made only of a subset of all fields, namely ϕ^{AB} , λ_α^A and $F_{\alpha\beta}$. It is an important fact that the algebra of the Q -generators closes off shell on the chiral part of \mathcal{T} [29], and hence these generators can be realised as differential operators. Of course, representing the \bar{Q} -generators in terms of differential operators is, in general, problematic, because the full supersymmetry algebra closes only on shell.

Moreover, for the chiral operator $\mathcal{T}(x, \theta^+)$ we have broken \bar{Q}^- since we have set $\theta^- = 0$ and hence we do not have a representation for this operator. For the Q_\pm -variation of $\mathcal{T}(x, \theta^+)$ we have,

$$[Q_-, \mathcal{T}(x, \theta^+)] = 0 , \quad [Q_+, \mathcal{T}(x, \theta^+)] = i \frac{\partial}{\partial \theta^+} \mathcal{T}(x, \theta^+) . \quad (3.11)$$

Note that since we consider the chiral part of the stress-tensor multiplet we have set $\bar{\theta} = 0$ and hence we have dropped $\bar{\theta}$ dependent terms in the realisation of Q and \bar{Q} . Then the first relation is obvious since $\mathcal{T}(x, \theta^+)$ is independent of θ^- . This also makes manifest the fact that all component operators of $\mathcal{T}(x, \theta^+)$ are annihilated by Q_{-a}^α [29]. On the other hand, Q_{+a}^α relates different components of the supermultiplet, as the second relation in (3.11) shows.

We define the super form factor as the super Fourier transform of the matrix element $\langle 1 \cdots n | \mathcal{T}(x, \theta^+) | 0 \rangle$, i.e.

$$\mathcal{F}_\mathcal{T}(q, \gamma_+; 1, \dots, n) := \int d^4x d^4\theta^+ e^{-(iqx + i\theta_\alpha^{+a} \gamma_{+a}^\alpha)} \langle 1 \cdots n | \mathcal{T}(x, \theta^+) | 0 \rangle , \quad (3.12)$$

where γ_{+a}^α is the Fourier-conjugate variable to θ_α^{+a} . Note that there is no γ_{-a}^α variable, since θ_α^{-a} has been set to zero in order to define the chiral part of the stress-tensor multiplet. The Ward identities (3.10) can then be recast as

$$\begin{aligned} \left(\sum_{i=1}^n \lambda_i \eta_{-,i} \right) \mathcal{F}_\mathcal{T}(q, \gamma_+; 1, \dots, n) &= 0 , \\ \left(\sum_{i=1}^n \lambda_i \eta_{+,i} - \gamma_+ \right) \mathcal{F}_\mathcal{T}(q, \gamma_+; 1, \dots, n) &= 0 , \end{aligned} \quad (3.13)$$

⁵We would like to thank Paul Heslop for a useful conversation on these issues.

where we have also introduced

$$\eta_{\pm a, i} := \bar{u}_{\pm a}^A \eta_{A, i} . \quad (3.14)$$

In arriving at (3.13) we have used (3.11) as well as the second relation in (3.2). Next, we observe that (3.13) are solved by

$$\mathcal{F}_{\mathcal{T}}(q, \gamma_+; 1, \dots, n) = \delta^{(4)}(q - \sum_{i=1}^n \lambda_i \tilde{\lambda}_i) \delta^{(4)}(\gamma_+ - \sum_{i=1}^n \eta_{+, i} \lambda_i) \delta^{(4)}(\sum_{i=1}^n \eta_{-, i} \lambda_i) R, \quad (3.15)$$

for some function R which in principle depends on all bosonic and fermionic variables. The simplest example is that of the MHV form factor, where the function R has a particularly simple expression derived in [18], namely

$$R^{\text{MHV}} = \frac{1}{\langle 12 \rangle \cdots \langle n1 \rangle} . \quad (3.16)$$

Notice that for an N^k MHV form factor, R has fermionic degree $4k$.

We can further constrain R by using some of the \bar{Q} -supersymmetries. More precisely, an inspection of the supersymmetry transformations of the fields reveals that a \bar{Q}^- transformation on the chiral part of the stress-tensor multiplet produces operators which are part of the full stress-tensor multiplet but not of its chiral truncation. Also, since $[Q_-, \mathcal{T}(x, \theta^+)] = 0$ we cannot realise \bar{Q}^- such that its anticommutator with Q_- gives a translation. One could of course still write a Ward identity for \bar{Q}^- , but this would involve operators of the full multiplet.

On the other hand, the \bar{Q}^+ -supersymmetry charge moves in the opposite direction of Q_+ across the different components of $\mathcal{T}(x, \theta^+)$, and is therefore realised as $\bar{Q}_\alpha^+ = -\theta^{+\alpha} \partial / \partial x^{\dot{\alpha}\alpha}$.

We should stress at this point that the supersymmetry algebra on component fields closes only up to equations of motion and gauge transformations (the latter drop out since we consider gauge invariant operators). An important exception is the subalgebra formed by the Q 's alone which does close off-shell for the fields appearing in $\mathcal{T}(x, \theta^+)$ [29]. Now we use the fact that matrix elements of terms proportional to equations of motion vanish at tree level, to argue that for our tree-level form factors the algebra formed by Q_+ and \bar{Q}^+ does close and, therefore, can be realised in the fashion described above. Thus, we can consider the \bar{Q}^+ Ward identity, which gives, after integrating by parts and using the third relation of (3.2),

$$\left(\sum_{i=1}^n \tilde{\lambda}_i \frac{\partial}{\partial \eta_{+, i}} - q \frac{\partial}{\partial \gamma_+} \right) \mathcal{F}_{\mathcal{T}}(q, \gamma_+; 1, \dots, n) = 0 . \quad (3.17)$$

Acting on (3.15), we obtain the following relation for R ,

$$\delta^{(4)}(q - \sum_{i=1}^n \lambda_i \tilde{\lambda}_i) \delta^{(4)}(\gamma_+ - \sum_{i=1}^n \eta_{+, i} \lambda_i) \delta^{(4)}(\sum_{i=1}^n \eta_{-, i} \lambda_i) \left[\left(\sum_{i=1}^n \tilde{\lambda}_i \frac{\partial}{\partial \eta_{+, i}} - q \frac{\partial}{\partial \gamma_+} \right) R \right] = 0 . \quad (3.18)$$

Notice that (3.18) implies a realisation of the supersymmetry generators on the form factor as

$$Q_{+a}^\alpha = \sum_{i=1}^n \lambda_i^\alpha \eta_{+a,i} - \gamma_{+a}^\alpha, \quad Q_{-a}^\alpha = \sum_{i=1}^n \lambda_i^\alpha \eta_{-a,i}, \quad (3.19)$$

whereas for $\bar{Q}_{\dot{\alpha}}^{+a}$,

$$\bar{Q}_{\dot{\alpha}}^{+a} = \sum_{i=1}^n \tilde{\lambda}_{i,\dot{\alpha}} \frac{\partial}{\partial \eta_{+a,i}} - q_{\alpha\dot{\alpha}} \frac{\partial}{\partial \gamma_{\alpha+a}}. \quad (3.20)$$

3.2 Examples

In the previous section we have derived the general form of the supersymmetric form factor defined in (3.12). This expression is given in (3.15), and was obtained by solving Ward identities related to translations and Q_\pm -supersymmetries. The use of \bar{Q}^+ supersymmetry led to the constraint (3.18) on the function R . For the sake of illustration, we now present a few examples of component form factors derived from (3.15).

3.2.1 Form factor of $\text{Tr}(\phi^{++}\phi^{++})$

Our first example is the form factor of $\text{Tr}(\phi^{++}\phi^{++})$, which appears as the $(\theta^+)^0$ -term in the expansion of $\mathcal{T}(x, \theta^+)$ in (3.3). In this case, since

$$\int d^4\theta^+ e^{i\theta_{\dot{\alpha}}^{+a}\gamma_{+a}^{\dot{\alpha}}} = (\gamma_+)^4, \quad (3.21)$$

we need to extract the $(\gamma_+)^4$ component of (3.15). This gives

$$\int d^4x e^{-iqx} \langle 1 \cdots n | \text{Tr}(\phi^{++}\phi^{++})(x) | 0 \rangle = \delta^{(4)}(q - \sum_{i=1}^n \lambda_i \tilde{\lambda}_i) \delta^{(4)}(\sum_{i=1}^n \eta_{-a,i} \lambda_i^\alpha) R, \quad (3.22)$$

or

$$\langle 1 \cdots n | \text{Tr}(\phi^{++}\phi^{++})(0) | 0 \rangle = \delta^{(4)}(\sum_{i=1}^n \eta_{-a,i} \lambda_i^\alpha) R. \quad (3.23)$$

Notice that with the help of (3.23) we can rewrite the supersymmetric form factor $\mathcal{F}_{\mathcal{T}}(q, \gamma_+; 1, \dots, n)$ as

$$\mathcal{F}_{\mathcal{T}}(q, \gamma_+; 1, \dots, n) = \delta^{(4)}(q - \sum_{i=1}^n \lambda_i \tilde{\lambda}_i) \delta^{(4)}(\gamma_+ - \sum_{i=1}^n \eta_{+,i} \lambda_i) \langle 1 \cdots n | \mathcal{T}(0, 0) | 0 \rangle, \quad (3.24)$$

since $\mathcal{T}(0,0) := \text{Tr}(\phi^{++}\phi^{++})(0)$. In other words, the function R appearing in the $\mathcal{T}(x, \theta^+)$ form factor can be calculated from the form factor of its lowest component⁶ $\text{Tr}(\phi^{++}\phi^{++})(0)$. Similar considerations apply to form factors of other half BPS operators such as $\text{Tr}(\phi^{++})^n$ with $n > 2$.

3.2.2 Form factor of the on-shell Lagrangian

As a second important example, we now consider the form factor for the on-shell Lagrangian, whose expression is [29]

$$\mathcal{L} = \text{Tr} \left[-\frac{1}{2} F_{\alpha\beta} F^{\alpha\beta} + \sqrt{2} g \lambda^{\alpha A} [\phi_{AB}, \lambda_{\alpha}^B] - \frac{1}{8} g^2 [\phi^{AB}, \phi^{CD}] [\phi_{AB}, \phi_{CD}] \right]. \quad (3.25)$$

Notice that it contains the self-dual part of $\text{Tr}(F^2)$. The on-shell Lagrangian appears as the $(\theta^+)^4$ coefficient of the expansion of $\mathcal{T}(x, \theta^+)$ in (3.3). The corresponding Fourier transform gives

$$\int d^4\theta^+ e^{-i\theta^+_{\alpha} \gamma^{\alpha}_{+a} (\theta^+)^4} = 1, \quad (3.26)$$

i.e. we have to take the $\mathcal{O}(\gamma^0)$ component of (3.15). This is simply

$$\langle 1 \cdots n | \mathcal{L}(0) | 0 \rangle = \delta^{(8)} \left(\sum_{i=1}^n \eta_i \lambda_i \right) \cdot R. \quad (3.27)$$

It is interesting to note that for an MHV form factor, (3.27) is formally identical to the tree-level MHV superamplitude, except for a delta function of momentum conservation which now imposes $\sum_i p_i = q$ rather than the usual momentum conservation of the particles. This allows us to make an interesting observation for the limit $q \rightarrow 0$ in which this form factor reduces simply to the corresponding scattering amplitude. Actually, it turns out that any form factor with the on-shell Lagrangian \mathcal{L} inserted reduces to the corresponding scattering amplitude in the $q \rightarrow 0$ limit, since the insertion of the action corresponds to differentiating the path-integral for the amplitude with respect to the coupling [42–44].

Another observation is that for the case of a gluonic state with MHV helicity configuration, (3.27) agrees with the Higgs plus multi-gluon or “ ϕ -MHV” amplitude considered in [45]. Indeed, if we have a gluonic state, we can effectively replace the on-shell Lagrangian (3.25) with its first term, the square of the self-dual field strength.

⁶One could arrive at (3.24) in a much more straightforward way by noticing that $\mathcal{T}(x, \theta^+_{\alpha}) = \exp(i\mathcal{P}x) \exp(iQ^{\alpha}_{+a} \theta^+_{\alpha}) \mathcal{T}(0,0) \exp(-i\mathcal{P}x) \exp(-iQ^{\alpha}_{+a} \theta^+_{\alpha})$ and using the invariance of the vacuum under supersymmetry and translations.

3.2.3 Why is the maximally non-MHV form factor so simple?

The simplest tree-level form factor is the MHV form factor, e.g.

$$\langle 1^+ 2^+ \dots i^- \dots j^- \dots (n-1)^+ n^+ | \text{Tr}(F_{\text{SD}}^2)(0) | 0 \rangle = \frac{\langle ij \rangle^4}{\langle 12 \rangle \langle 23 \rangle \dots \langle n-1 \rangle} . \quad (3.28)$$

Interestingly, there are non-MHV form factors whose expression is also remarkably simple. Consider for example that of the self-dual field strength with an all negative-helicity gluons state – we refer to this as the “maximally non-MHV” form factor. The result for this quantity is [45]

$$\langle 1^- \dots n^- | \text{Tr}(F_{\text{SD}}^2)(0) | 0 \rangle = \frac{q^4}{[1\ 2][2\ 3] \dots [n\ 1]} . \quad (3.29)$$

In the following we wish to show that the simplicity of (3.29) is determined by the supersymmetric Ward identity discussed earlier, and is linked to that of the MHV super form factor (3.16).

Recall from (3.24) that the super form factor of the chiral part of the stress-tensor multiplet $\mathcal{T}(x, \theta^+)$ has the form

$$\mathcal{F}_{\mathcal{T}} = \delta^{(4)}(q - \sum_{i=1}^n \lambda_i \tilde{\lambda}_i) \delta^{(4)}(\gamma_+ - \sum_{i=1}^n \eta_{+,i} \lambda_i) \mathcal{F}_{\phi^2} , \quad (3.30)$$

where

$$\mathcal{F}_{\phi^2} := \langle 1 \dots n | \text{Tr}(\phi^{++} \phi^{++})(0) | 0 \rangle = \delta^{(4)}\left(\sum_{i=1}^n \eta_{-,i} \lambda_i\right) R . \quad (3.31)$$

For the MHV helicity configuration, the function R^{MHV} is given in (3.16),

$$\mathcal{F}_{\phi^2}^{\text{MHV}} = \frac{\delta^{(4)}\left(\sum_{i=1}^n \eta_{-,i} \lambda_i\right)}{\langle 12 \rangle \dots \langle n1 \rangle} . \quad (3.32)$$

We can now use this fact and perform a Grassmann Fourier transform in order to derive the maximally non-MHV super form factor,

$$\mathcal{F}_{\phi^2}^{\text{N}^{\text{max}}\text{MHV}} = \prod_{i=1}^n \int d^4 \tilde{\eta}_i e^{i \eta_{i,A} \tilde{\eta}_i^A} \frac{\delta^{(4)}\left(\sum_{i=1}^n \tilde{\eta}_i^+ \tilde{\lambda}_i\right)}{[12] \dots [n1]} . \quad (3.33)$$

Thus, the maximally non-MHV super form factor for the chiral part of the stress-tensor multiplet is

$$\mathcal{F}_{\mathcal{T}}^{\text{N}^{\text{max}}\text{MHV}} = \delta^{(4)}(q - \sum_{i=1}^n \lambda_i \tilde{\lambda}_i) \delta^{(4)}(\gamma_+ - \sum_{i=1}^n \eta_{+,i} \lambda_i) \mathcal{F}_{\phi^2}^{\text{N}^{\text{max}}\text{MHV}} . \quad (3.34)$$

We now focus on the component corresponding to the self-dual field strength, which can be obtained from the coefficient of $(\gamma_+)^0$. This is given by⁷

$$\begin{aligned}
& \delta^{(4)} \left(\sum_{i=1}^n \eta_{+,i} \lambda_i \right) \prod_{i=1}^n \int d^4 \tilde{\eta}_i e^{i \eta_i \tilde{\eta}_i} \frac{\delta^{(4)} \left(\sum_{i=1}^n \tilde{\eta}_i^+ \tilde{\lambda}_i \right)}{[12] \cdots [n1]} \\
&= \delta^{(4)} \left(\sum_{i=1}^n \eta_{+,i} \lambda_i \right) \frac{\sum_{i < j} [ij] \sum_{k < l} [kl]}{[12] \cdots [n1]} \eta_1^4 \cdots \eta_i^3 \cdots \eta_j^3 \cdots \eta_k^3 \cdots \eta_l^3 \cdots \eta_n^4 \\
&= \frac{\sum_{i < j} \langle ij \rangle [ij] \sum_{k < l} \langle kl \rangle [kl]}{[12] \cdots [n1]} \eta_1^4 \cdots \eta_n^4 \\
&= \frac{q^4}{[12] \cdots [n1]} \eta_1^4 \cdots \eta_n^4. \tag{3.35}
\end{aligned}$$

Equation (3.35) shows that there is a non-vanishing maximally non-MHV form factor for the self-dual field strength, whose expression is precisely given by (3.29).

3.3 Form factor of the complete stress-tensor multiplet

In this section we consider the form factor of the the full, non-chiral stress-tensor multiplet $\mathcal{T}(x, \theta^+, \tilde{\theta}_-)$. We can write this as⁸

$$\begin{aligned}
\mathcal{T}(x, \theta^+, \tilde{\theta}_-) &:= \text{Tr}(W^{++} W^{++}) \\
&= e^{i\theta^+ Q_+ + i\tilde{\theta}_- \bar{Q}^-} \text{Tr}(\phi^{++} \phi^{++})(x) e^{-i\theta^+ Q_+ - i\tilde{\theta}_- \bar{Q}^-} \\
&= \text{Tr}(\phi^{++} \phi^{++}) + (\theta^+)^4 \mathcal{L} + (\tilde{\theta}_-)^4 \tilde{\mathcal{L}} + (\theta^+ \sigma^\mu \tilde{\theta}_-) (\theta^+ \sigma^\nu \tilde{\theta}_-) T_{\mu\nu} + \cdots, \tag{3.36}
\end{aligned}$$

where we have indicated only some terms of the full multiplet.

The right-hand side of (3.36) is an expansion in the chiral as well as anti-chiral variables θ^+ and $\tilde{\theta}_-$. We can parallel this feature in the states by using a non-chiral description as in [46] with fermionic variables η_+ and $\tilde{\eta}_-$. With this choice, the supersymmetry algebra is realised on states as

$$\begin{aligned}
\langle i | Q_+ &= \langle i | \lambda_i \eta_{+,i}, & \langle i | Q_- &= \langle i | \lambda_i \frac{\partial}{\partial \tilde{\eta}_i^-}, \\
\langle i | \bar{Q}^- &= \langle i | \tilde{\lambda}_i \tilde{\eta}_i^-, & \langle i | \bar{Q}^+ &= \langle i | \tilde{\lambda}_i \frac{\partial}{\partial \eta_{+,i}}. \tag{3.37}
\end{aligned}$$

This non-chiral representation can be obtained via a simple Fourier transform of half of the chiral superspace variables. In terms of the Nair description of states, this

⁷In the following equation we omit a trivial delta function of momentum conservation.

⁸Notice that the second equality is true only up to equations of motion because the non-chiral algebra closes only on shell. In the following we will work at tree level and hence this point will not affect our considerations.

amounts to introducing a new super wavefunction,

$$\begin{aligned}\Phi(p, \eta_+, \tilde{\eta}^-) &:= \int d^2 \eta_- e^{i\eta_- \tilde{\eta}^-} \Phi(p, \eta) \\ &= g^+(p)(\tilde{\eta}^-)^2 + \cdots + \phi^{++}(\eta_+)^2(\tilde{\eta}^-)^2 + \phi^{--} + \cdots + g^-(p)(\eta_+)^2.\end{aligned}\quad (3.38)$$

As a result, operators and superstates live in a non-chiral superspace. The non-chiral form factor in this representation is defined as

$$\mathcal{F}(q, \gamma_+, \tilde{\gamma}^-; 1, \dots, n) := \int d^4 x d^4 \theta^+ d^4 \tilde{\theta}_- e^{-i(qx + \theta^+ \gamma_+ + \tilde{\theta}_- \tilde{\gamma}^-)} \langle 1 \dots n | \mathcal{T}(x, \theta^+, \tilde{\theta}_-) | 0 \rangle. \quad (3.39)$$

In order to write down Ward identities for (3.39), we consider the action of supersymmetry generators on the operator $\mathcal{T}(x, \theta^+, \tilde{\theta}_-)$:

$$\begin{aligned}[Q_+, \mathcal{T}(x, \theta^+, \tilde{\theta}_-)] &= i \frac{\partial}{\partial \theta^+} \mathcal{T}(x, \theta^+, \tilde{\theta}_-), \quad [Q_-, \mathcal{T}(x, \theta^+, \tilde{\theta}_-)] = -\tilde{\theta}_- \frac{\partial}{\partial x} \mathcal{T}(x, \theta^+, \tilde{\theta}_-), \\ [\bar{Q}^-, \mathcal{T}(x, \theta^+, \tilde{\theta}_-)] &= -\frac{\partial}{\partial \tilde{\theta}_-} \mathcal{T}(x, \theta^+, \tilde{\theta}_-), \quad [\bar{Q}^+, \mathcal{T}(x, \theta^+, \tilde{\theta}_-)] = i\theta^+ \frac{\partial}{\partial x} \mathcal{T}(x, \theta^+, \tilde{\theta}_-).\end{aligned}\quad (3.40)$$

Following closely the derivation of the Ward identities described in the previous section, we arrive at the following relations for each supersymmetry generator,

$$Q_+ : \quad (\eta_+ \lambda - \gamma_+) \mathcal{F} = 0, \quad Q_- : \quad \left(q \frac{\partial}{\partial \tilde{\gamma}^-} - \lambda \frac{\partial}{\partial \tilde{\eta}^-} \right) \mathcal{F} = 0, \quad (3.41)$$

$$\bar{Q}^- : \quad (\tilde{\eta}^- \tilde{\lambda} - \tilde{\gamma}^-) \mathcal{F} = 0, \quad \bar{Q}^+ : \quad \left(q \frac{\partial}{\partial \gamma_+} - \tilde{\lambda} \frac{\partial}{\partial \eta_+} \right) \mathcal{F} = 0, \quad (3.42)$$

and hence the form factor in (3.39) takes the form

$$\mathcal{F} = \delta^{(4)}(q - \sum_{i=1}^n \lambda_i \tilde{\lambda}_i) \delta^{(4)}(\gamma_+ - \sum_{i=1}^n \eta_{+,i} \lambda_i) \delta^{(4)}(\tilde{\gamma}^- - \sum_{i=1}^n \tilde{\eta}_i^- \tilde{\lambda}_i) \mathcal{F}_{\phi^2}^{\text{nc}}, \quad (3.43)$$

for some function $\mathcal{F}_{\phi^2}^{\text{nc}}$.

A useful observation is that $\mathcal{F}_{\phi^2}^{\text{nc}}$ can be obtained from the corresponding function introduced in (3.30) for the chiral form factor via a half-Fourier transform on the η and $\tilde{\eta}$ variables, as

$$\mathcal{F}_{\phi^2}^{\text{nc}}(\lambda, \tilde{\lambda}, \eta_+, \tilde{\eta}^-) = \prod_{i=1}^n \int d^2 \eta_{-,i} e^{i\eta_{-,i} \tilde{\eta}_i^-} \mathcal{F}_{\phi^2}(\lambda, \tilde{\lambda}, \eta_+, \eta_-). \quad (3.44)$$

In the remaining part of this section we would like to show a few applications of this formulation.

To begin with, we specialise to the MHV case, for which we have

$$\begin{aligned}\mathcal{F}_{\phi^2}^{\text{MHV,nc}} &= \prod_{i=1}^n \int d^2\eta_{-,i} e^{i\eta_{-,i}\tilde{\eta}_i^-} \frac{\delta^{(4)}(\sum_{i=1}^n \eta_{-,i}\lambda_i)}{\langle 12 \rangle \cdots \langle n1 \rangle} \\ &= \frac{\langle kl \rangle^2}{\langle 12 \rangle \cdots \langle n1 \rangle} \prod_{i \neq k,l}^n (\tilde{\eta}_i^-)^2 + \cdots .\end{aligned}\quad (3.45)$$

The MHV form factor of $\text{Tr}(\phi^+)^2$ is then obtained by extracting the coefficient of $(\gamma_+)^4(\tilde{\gamma}^-)^4$ in (3.43), and thus it is immediately seen to give the correct answer. The form factor with an insertion of the chiral Lagrangian \mathcal{L} (which includes $\text{Tr}(F_{\text{SD}}^2)$) is obtained by taking the coefficient of $(\gamma_+)^0(\tilde{\gamma}^-)^4$:

$$\mathcal{F}_{\mathcal{L}}^{\text{MHV}} = \delta^{(4)}\left(\sum_{i=1}^n \eta_{+,i}\lambda_i\right) \mathcal{F}_{\phi^2}^{\text{MHV}} = \frac{\langle kl \rangle^4}{\langle 12 \rangle \cdots \langle n1 \rangle} \left(\eta_{+,k}^2 \eta_{+,l}^2 \prod_{i \neq k,l}^n (\tilde{\eta}_i^-)^2 \right) + \cdots , \quad (3.46)$$

as expected. Finally, in order to obtain the form factor with $\tilde{\mathcal{L}}$ (which includes $\text{Tr}(F_{\text{ASD}}^2)$), we extract the coefficient of $(\gamma_+)^4(\tilde{\gamma}^-)^0$:

$$\begin{aligned}\mathcal{F}_{\tilde{\mathcal{L}}}^{\text{MHV}} &= \delta^{(4)}\left(\sum_{i=1}^n \tilde{\eta}_i^- \tilde{\lambda}_i\right) \mathcal{F}_{\phi^2}^{\text{MHV}} = \frac{\sum_{i < j} \langle ij \rangle [ij] \sum_{k < l} \langle kl \rangle [kl]}{\langle 12 \rangle \cdots \langle n1 \rangle} \prod_{i=1}^n (\tilde{\eta}_i^-)^2 \\ &= \frac{q^4}{\langle 12 \rangle \cdots \langle n1 \rangle} \prod_{i=1}^n (\tilde{\eta}_i^-)^2 ,\end{aligned}\quad (3.47)$$

which is indeed also correct.

4 Supersymmetric methods

In this section we take a brief survey of various methods that can be used to calculate form factors of the complete stress-tensor multiplet, at tree and loop level. These are simple but interesting extensions of well-known techniques for scattering amplitudes – MHV diagrams [21], on-shell recursion relations [22, 23] and (generalised) unitarity [47–50] – thus we will limit ourselves to highlighting the peculiarities we encounter when dealing with form factors. The non-supersymmetric versions of these methods have been considered earlier in Section 2 and in [18].

A preliminary observation is that the form factor of the complete stress-tensor multiplet operator $\mathcal{T}(x, \theta^+, \tilde{\theta}_-)$ can be expressed in terms of that of its lowest bosonic component $\text{Tr}(\phi^{++}\phi^{++})$, as we have shown in (3.43), namely

$$\mathcal{F} = \delta^{(4)}\left(q - \sum_{i=1}^n \lambda_i \tilde{\lambda}_i\right) \delta^{(4)}\left(\gamma_+ - \sum_{i=1}^n \eta_{+,i}\lambda_i\right) \delta^{(4)}\left(\tilde{\gamma}^- - \sum_{i=1}^n \tilde{\eta}_i^- \tilde{\lambda}_i\right) \mathcal{F}_{\phi^2}^{\text{nc}} , \quad (4.1)$$

where $\mathcal{F}_{\phi^2}^{\text{nc}} := \langle 1 \cdots n | \text{Tr}(\phi^{++} \phi^{++})(0) | 0 \rangle$ and the superstate $\langle 1 \cdots n |$ is here in the non-chiral representation. One can then switch instantly to the chiral representation via a half-Fourier transform from the $\tilde{\eta}^-$ to the η_+ variables. Hence, we only need to devise methods to calculate the form factor $\langle 1 \cdots n | \text{Tr}(\phi^{++} \phi^{++})(0) | 0 \rangle$ using a chiral representation for the external state. This is the problem we address in the following.⁹

4.1 Supersymmetric MHV rules

We begin with a lightning illustration of super MHV rules. Here, the super MHV form factor,

$$\mathcal{F}^{\text{MHV}}(1, 2, \dots, n; q) = \frac{\delta^{(4)}(q - \sum_i \lambda_i \tilde{\lambda}_i) \delta^{(4)}(\sum_i \lambda_i \eta_{i,-})}{\langle 1 \ 2 \rangle \langle 2 \ 3 \rangle \cdots \langle n \ 1 \rangle}, \quad (4.2)$$

is continued off shell with the standard prescription (2.4) of [21], and used as a vertex in addition to the standard MHV vertices. Form factors have a single operator insertion, hence we only draw diagrams with a single form factor MHV vertex. As an example, consider the NMHV tree-level super form factor. It can be computed by summing over all diagrams in Figure 5(a), whose expression is

$$\begin{aligned} \mathcal{F}_{\text{NMHV}}^{(0)} &= \sum_{i=1}^n \sum_{j=i+1}^{i+n-2} \int d^4 P_{ij} \int d^4 \eta_P \mathcal{A}_{\text{MHV}}^{(0)}(i, \dots, j, P_{ij}) \frac{1}{P_{ij}^2} \mathcal{F}_{\text{MHV}}^{(0)}(j+1, \dots, i-1, -P_{ij}; q) \\ &= \mathcal{F}_{\text{MHV}}^{(0)} \sum_{i=1}^n \sum_{j=i+1}^{i+n-2} \frac{\langle i-1 \ i \rangle \langle j \ j+1 \rangle}{\langle i-1 \ P_{ij} \rangle \langle P_{ij} \ i \rangle \langle j \ P_{ij} \rangle \langle P_{ij} \ j+1 \rangle} \frac{1}{P_{ij}^2} \delta^{(4)}\left(\sum_{k=i}^j \langle P_{ij} \ k \rangle \eta_k^A\right). \end{aligned} \quad (4.3)$$

We have also calculated tree-level N²MHV super form factor up to six points and checked that the results are all independent of the choice of reference spinor. We have also re-derived the split-helicity form factors, and checked numerical agreement with the results presented in Section 2.2.1.

As an additional example, consider the one-loop MHV super form factor. Following [36], this can be computed by summing over all diagrams in Figure 5(b), and is given by

$$\begin{aligned} \mathcal{F}_{\text{MHV}}^{(1)} &= \sum_{i=1}^n \sum_{j=i}^{i+n-1} \int \frac{d^D L_1}{L_1^2 + i\varepsilon} \frac{d^D L_2}{L_2^2 + i\varepsilon} \int d^4 \eta_{L_1} \int d^4 \eta_{L_2} \\ &\quad \mathcal{A}_{\text{MHV}}^{(0)}(i \dots, j, L_1, L_2) \mathcal{F}_{\text{MHV}}^{(0)}(-L_2, -L_1, j+1, \dots, i-1; q). \end{aligned} \quad (4.4)$$

Finally, we note that the MHV vertex expansion may be proved at tree level along the lines of [51], namely by using a BCFW recursion relation with an all-line shift and showing that this is identical to the MHV diagram expansion.

⁹To simplify our notation, we will drop from now on the subscript in \mathcal{F}_{ϕ^2} .

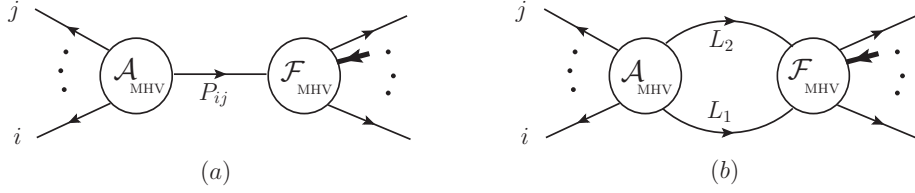


Figure 5: (a) *MHV diagram for a tree-level NMHV form factor.* (b) *MHV diagram for a one-loop MHV form factor.*

4.2 Supersymmetric recursion relations

Now we consider a simple extension of the supersymmetric version [52, 53] of the BCFW recursion relation [22, 23]. We choose to work with an $[i, j]$ shift, $\tilde{\lambda}_i \rightarrow \tilde{\lambda}_i + z\tilde{\lambda}_j$, $\lambda_j \rightarrow \lambda_j - z\lambda_i$, $\eta_i \rightarrow \eta_i + z\eta_j$. Factorisation requires that each term in the recursion relation must contain one form factor and one amplitude. Hence, for each kinematic channel we need to sum over two diagrams, with the form factor appearing either on the left-hand or right-hand side, see Figure 6. The result one obtains by summing over these two classes of diagrams has the form

$$\begin{aligned} \mathcal{F}(0) &= \sum_{a,b} \int d^4P d^4\eta_P \mathcal{F}_L(z=z_{ab}) \frac{1}{P_{ab}^2} \mathcal{A}_R(z=z_{ab}) \\ &+ \sum_{c,d} \int d^4P d^4\eta_P \mathcal{A}_L(z=z_{cd}) \frac{1}{P_{cd}^2} \mathcal{F}_R(z=z_{cd}) . \end{aligned} \quad (4.5)$$

One point deserves a special attention, namely the large- z behaviour of the form

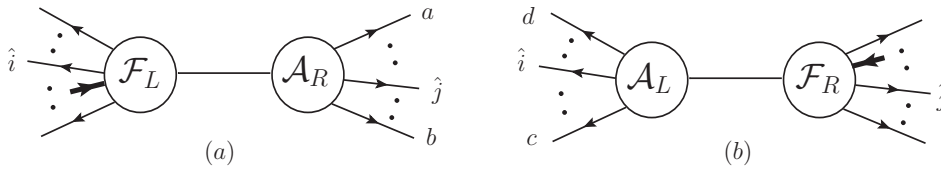


Figure 6: *The two recursive diagrams discussed in the text.*

factor. Recall that in order to have a recursion relation without boundary terms we need $\mathcal{F}(\dots \hat{p}_i, \dots, \hat{p}_j, \dots) \rightarrow 0$ as $z \rightarrow \infty$. We discuss this important point in Appendix A, where we prove that the condition mentioned above is indeed satisfied. We would also like to point out that the basic seeds in the form factor recursion relation are the two-point form factor, together with the three-point amplitudes.

4.3 Supersymmetric unitarity-based method

Supersymmetric generalised unitarity, as well as supersymmetric MHV rules, are easily applied to form factors. Consider for example a two-particle cut, depicted in Figure 7. On one side of the cut we have a tree-level form factor, on the other a tree scattering amplitude. For the case of a one-loop supersymmetric MHV form factor, the two-particle cut is equal to

$$\mathcal{F}_{\text{MHV}}^{(1)} \Big|_{s_{a+1,b-1}\text{-cut}} = \int d\text{LIPS}(l_1, l_2; P) \int d^4\eta_{l_1} \int d^4\eta_{l_2} \mathcal{F}_{\text{MHV}}^{(0)}(-l_2, -l_1, b, \dots, a; q) \mathcal{A}_{\text{MHV}}^{(0)}(l_1, l_2, (a+1) \dots, (b-1)) , \quad (4.6)$$

where the Lorentz-invariant phase-space measure is

$$d\text{LIPS}(l_1, l_2; P) := d^D l_1 d^D l_2 \delta^+(l_1^2) \delta^+(l_2^2) \delta^D(l_1 + l_2 + P) . \quad (4.7)$$

The sum over all possible states which can propagate in the loop is automatically

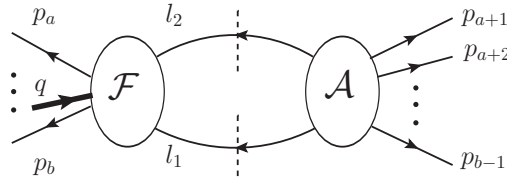


Figure 7: A two-particle cut diagram for a one-loop form factor.

performed by the fermionic integration. A simple calculation gives

$$\mathcal{F}_{\text{MHV}}^{(1)} \Big|_{s_{a+1,b-1}\text{-cut}} = \mathcal{F}_{\text{MHV}}^{(0)} \int d\text{LIPS}(l_1, l_2; P_{a+1,b-1}) \frac{\langle a a+1 \rangle \langle l_2 l_1 \rangle}{\langle a l_2 \rangle \langle l_2 a+1 \rangle} \frac{\langle b-1 b \rangle \langle l_1 l_2 \rangle}{\langle b-1 l_1 \rangle \langle l_1 b \rangle} , \quad (4.8)$$

which reproduces the result derived in [18] using component form factors and amplitudes.

5 Dual MHV rules for form factors

It was shown in [54] that the expectation value of supersymmetric Wilson loops in momentum twistor space generates all planar amplitudes in $\mathcal{N} = 4$ SYM, and dual MHV rules in momentum twistor space were proposed in [55]. Inspired by these results, dual MHV rules directly formulated in dual momentum space were introduced in [56]. In these rules a lightlike closed polygon formed by linking the on-shell momenta of the external particles following their colour ordering plays an important role. Note that the same polygon appears in the amplitude/Wilson loop duality [32–34].

In this section we extend these rules to the calculation of form factors of the special operator considered in previous sections, namely the chiral part of the stress-tensor multiplet operator. It turns out that the rules for the amplitude have to be modified only slightly. More precisely, there are no new vertices to be introduced, and we only have to modify (super)momentum conservation of the particles in order to account for the (super)momentum injected by the operator. In the dual momentum picture, this implies the breaking of the closed null contour describing the particle's momenta.

The vertices of this open polygon in dual supermomentum space are labelled by (x_i, Θ_i) [57], with¹⁰

$$x_i - x_{i+1} := p_i = \lambda_i \tilde{\lambda}_i, \quad \Theta_i - \Theta_{i+1} := \lambda_i \eta_i, \quad (5.1)$$

with

$$x_i - x_{i+n} = \sum_{j=1}^n p_j = q, \quad \Theta_i - \Theta_{i+n} = \sum_{j=1}^n \lambda_j \eta_j = \gamma, \quad (5.2)$$

where q (γ) is the (super)momentum carried by the operator. Note that in the previous equation we have effectively injected the (super)momentum of the operator between on-shell states labelled by $i-1$ and i and this is where the breaking of the polygon occurs. For each diagram an appropriate choice for the location of the breaking will have to be made. Furthermore, in this section we consider the chiral operator $\mathcal{T}(x, \theta^+)$ for which $\gamma_- = 0$, and hence $\Theta_{i;-} - \Theta_{i+n;-} = 0$. For amplitudes we have of course $q = 0$ and $\gamma = 0$ which would bring us back to a closed lightlike polygon.

In practice it is useful to convert the open polygon for form factors into a periodic configuration in dual momentum space with period q (γ) in the bosonic (fermionic) direction as in Figure 8. This is partially motivated by a duality observed at strong coupling in [15, 16] where form factors are related to the area of minimal surfaces ending on an infinite periodic sequence of null segments at the boundary of AdS . In [18] an attempt was made to map this geometric picture to weak coupling, in a way similar to the amplitude/Wilson loop duality [33, 34].

The emergence of a periodic configuration is also natural from a field-theoretic point of view once one takes into account that the operator insertion is a colour singlet, and hence does not interfere with the colour ordering of the external state. In other words, the (super)momentum carried by the operator can be inserted between any pair of particle momenta without spoiling the ordering. Precisely by resorting to a periodic configuration we can account for this property, as Figure 8 clearly shows.

One can also consider this periodic kinematic configuration in momentum twistor space [58], as shown in Figure 9, with space-time points being mapped to lines in

¹⁰In order to avoid confusion with the variables θ 's introduced in earlier sections, we denote by Θ the variables living in dual super momentum space.

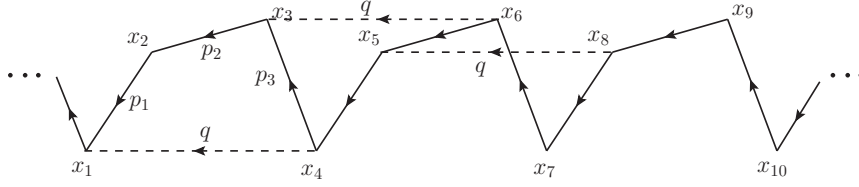


Figure 8: *The kinematic configuration in dual momentum space used to calculate three-point form factors using dual MHV rules.*

twistor space: $(x_i, \Theta_i) \sim \mathcal{Z}_{i-1} \wedge \mathcal{Z}_i$, where

$$\mathcal{Z}_i = (\lambda_i, \nu_i, \chi_i), \quad \nu_i = x_i \lambda_i = x_{i+1} \lambda_i, \quad \chi_i = \Theta_i \lambda_i = \Theta_{i+1} \lambda_i. \quad (5.3)$$

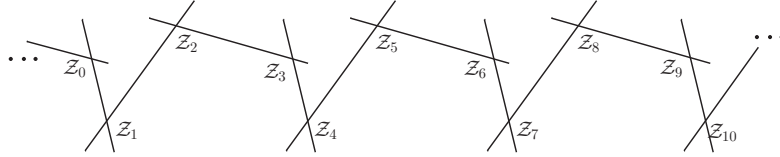


Figure 9: *The same kinematic configuration presented in Figure 8, in terms of momentum twistor space variables.*

5.1 Examples

In this section we want to explain the dual MHV rules by discussing a number of simple examples of tree-level and one-loop form factors. The dual MHV rules in dual momentum space for $\mathcal{N} = 4$ amplitudes are summarised for the reader's convenience in Appendix B, and we refer to [56] for full details.

The first example is that of an NMHV three-point form factor. The corresponding diagrams are shown in Figure 10, and are in one-to-one correspondence with three conventional MHV diagrams, depicted in Figure 11. Notice that the three diagrams in Figure 10 can be obtained by selecting the appropriate period in Figure 8.

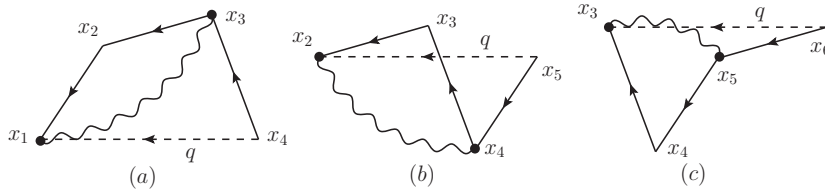


Figure 10: *Dual MHV diagrams for the three-point tree NMHV form factor.*

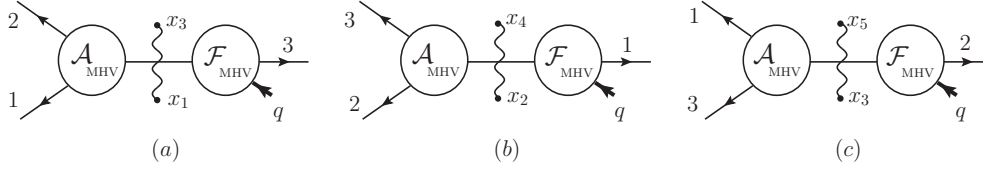


Figure 11: *Corresponding MHV diagrams for the three-point tree NMHV form factor.*

The extension to n -point NMHV form factors is immediate – we consider all dual MHV diagrams where one propagator connects two external vertices *within one period*. The final result is given by summing over all translationally inequivalent diagrams as

$$\mathcal{F}_{\text{NMHV}}^{(0)} = \mathcal{F}_{\text{MHV}}^{(0)} \sum_{i=1}^n \sum_{j=i+2}^{i+n-1} \frac{\langle i-1 \ i \rangle}{\langle i-1 \ \ell_{ij} \rangle \langle \ell_{ij} \ i \rangle} \frac{\langle j-1 \ j \rangle}{\langle j-1 \ \ell_{ij} \rangle \langle \ell_{ij} \ j \rangle} \frac{1}{x_{ij}^2} \int d^4 \eta_{ij} \delta^{0|8}(\ell_{ij} \eta_{ij} + \Theta_{ij}) , \quad (5.4)$$

where the spinor $|\ell_{ij}\rangle$ associated to the internal leg is defined as

$$|\ell_{ij}\rangle := |x_{ij}|\xi] , \quad (5.5)$$

and where $|\xi]$ is an arbitrary reference spinor. Notice that the particle labels of spinor variables i and $i+n$ are identified in this expression. Importantly, the fact that we are calculating a form factor rather than an amplitude – and the corresponding dependence on q and γ – is completely encoded in the periodic kinematic configuration as defined earlier. Furthermore, we observe that every diagram in the sum corresponds to a particular period (see Figures 10 and 11).

Notice that diagrams where a propagator connects two adjacent points give a vanishing result, and therefore are not included in the summation. On the other hand, diagrams where a propagator connects two points separated by exactly one period or more are non-vanishing, and have to be excluded since there is no corresponding conventional MHV diagram. For instance, among the three-point diagrams in Figure 10 we do not include the diagram with a propagator connecting points x_1 and x_4 . This is an example of a more general fact: *diagrams where a single propagator connects points x_i and x_j with $|i-j| \geq n$ have to be discarded*. This applies to any loop order. The reason for this rule is that there are no corresponding supersymmetric MHV diagrams.

As an aside we mention that (5.4) can also be written in terms of momentum twistor variables as

$$\mathcal{F}_{\text{NMHV}}^{(0)} = \mathcal{F}_{\text{MHV}}^{(0)} \sum_{i=1}^n \sum_{j=i+2}^{i+n-1} [*, i-1, i, j-1, j] , \quad (5.6)$$

where \mathcal{Z}_* is the reference momentum twistor, chosen as

$$\mathcal{Z}_* = (0, \xi, 0) , \quad (5.7)$$

and $[*, i-1, i, j-1, j]$ is defined in (B.4).

The case of one-loop MHV form factors is similar to the tree-level NMHV case. The n -point one-loop MHV form factor is given by

$$\begin{aligned}
\mathcal{F}_{\text{MHV}}^{(1)} &= \mathcal{F}_{\text{MHV}}^{(0)} \int d^4 x_I d^8 \Theta_I \sum_{i=1}^n \sum_{j=i+1}^{i+n-1} \frac{\langle i-1 \ i \rangle}{\langle i-1 \ \ell_{iI} \rangle \langle \ell_{iI} \ i \rangle} \frac{\langle j-1 \ j \rangle}{\langle j-1 \ \ell_{Ij} \rangle \langle \ell_{Ij} \ j \rangle} \\
&\quad \frac{1}{\langle \ell_{iI} \ell_{Ij} \rangle \langle \ell_{Ij} \ell_{iI} \rangle} \frac{1}{x_{iI}^2} \int d^4 \eta_{iI} \delta^{0|8}(\ell_{iI} \eta_{iI} + \Theta_{iI}) \frac{1}{x_{Ij}^2} \int d^4 \eta_{Ij} \delta^{0|8}(\ell_{Ij} \eta_{Ij} + \Theta_{Ij}) \\
&+ \mathcal{F}_{\text{MHV}}^{(0)} \int d^4 x_I d^8 \Theta_I \sum_{i=1}^n \frac{\langle i-1 \ i \rangle}{\langle i-1 \ \ell_{iI'} \rangle \langle \ell_{iI'} \ \ell_{iI} \rangle \langle \ell_{iI} \ i \rangle} \frac{1}{\langle \ell_{iI} \ell_{i+nI} \rangle \langle \ell_{i+nI} \ell_{iI} \rangle} \\
&\quad \frac{1}{x_{iI}^2} \int d^4 \eta_{iI} \delta^{0|8}(\ell_{iI} \eta_{iI} + \Theta_{iI}) \frac{1}{x_{i+nI}^2} \int d^4 \eta_{i+nI} \delta^{0|8}(\ell_{i+nI} \eta_{i+nI} + \Theta_{i+nI}) \\
&\quad \int d^4 x_{I'} d^8 \Theta_{I'} \delta^4(x_{I'I} - x_{i+nI}) \delta^{0|8}(\Theta_{I'I} - \Theta_{i+nI}) .
\end{aligned} \tag{5.8}$$

Notice that we have treated a special class of diagrams differently, corresponding to the last three lines in (5.8). These are diagrams where the two propagators have momenta x_{iI} and x_{i+nI} . An example of such a diagram in the case of a three-point form factor is shown in Figure 12.

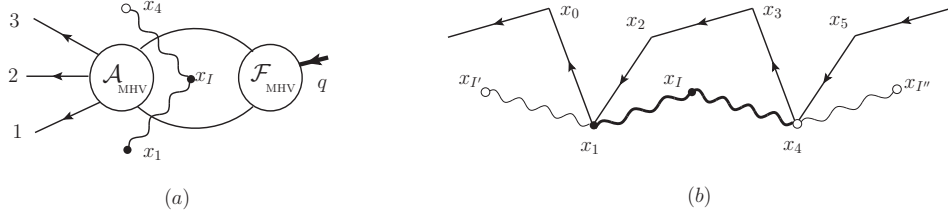


Figure 12: A special diagram with two propagators with momenta x_{iI} and x_{i+nI} . In the dual MHV diagram there are two propagators with momenta x_{1I} and x_{4I} , and two vertices, x_1 and x_I . Such diagrams correspond to the last three lines of (5.8).

The three-point dual MHV diagrams at one loop are shown in Figure 13. The diagrams in Figure 13 (g)-(i) are of the special class described earlier in Figure 12. Note that in the case of loop diagrams we also have to include diagrams where two adjacent points or two points separated by exactly one period are connected by two or more propagators (see Figure 13 diagrams (a)-(c) and (g)-(i) respectively). We should also stress that all diagrams where two points x_i and x_j with $|i-j| > n$ are connected must be discarded. Generalisations to non-MHV form factors are straightforward.

Finally we compare the dual MHV diagrams with the periodic Wilson line diagrams studied in [18]. We can see that an identical truncation was necessary in order to obtain the correct result: in a single MHV diagram the external vertices which are

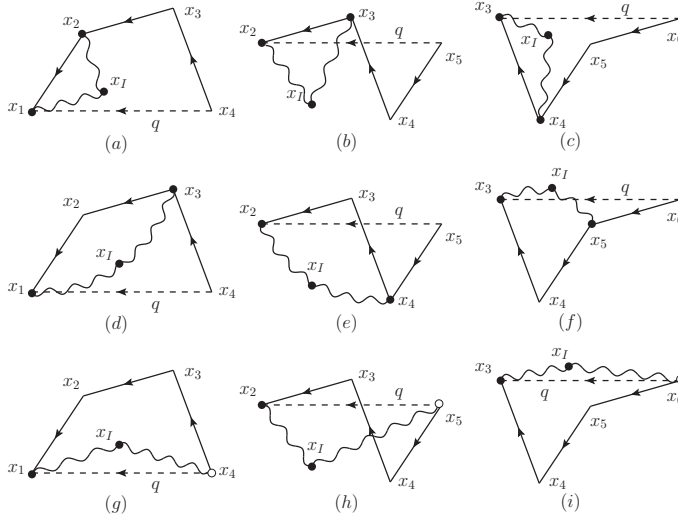


Figure 13: *Dual MHV diagrams for the three-point MHV form factor at one loop.*

connected to propagators must reside within one period, and the whole form factor is obtained by summing over all translationally inequivalent diagrams.

5.2 Higher-loop diagrams

At higher loops, the situation becomes more involved. To illustrate the main novelty we consider the two-point MHV form factor at two loops.¹¹

As prototypical examples, we consider two particular diagrams, depicted in Figures 14 and 15. In the first diagram, the form factor MHV vertex is inserted in the exterior part of the diagram, whereas in the second situation it is inserted in the interior. On the right-hand side of each figure we also draw the corresponding dual MHV diagram. Let us start with the first, simpler situation. There is no subtlety in defining the internal region momenta x_I and x_J . The momenta in the propagators in the outer loop are x_{2I} , x_{3J} and x_{1J} , and it is straightforward to write down the two-loop dual MHV integrand. In the notation of Appendix B, there are two internal vertices, two external vertices at x_1 and x_2 (with x_1 being a two-point vertex) and four propagators, as shown by dark bullets and dark wavy lines in Figure 14 (b).

Consider now the second, more subtle situation drawn in Figure 15. In order to assign region momenta consistently to all regions in this diagram, we need to introduce an additional loop momentum $x_{J'}$ such that $x_J - x_{J'} = q$, in exactly the same way as

¹¹Incidentally, we recall that while at one loop it has been proved that (four-dimensional) MHV diagrams reproduce complete amplitudes [59], there is no such statement at two loops and beyond. However, MHV diagrams at two loops and beyond can be used effectively to compute unregulated integrands of amplitudes (and form factors, as demonstrated here) which have recently attracted great interest in their own right [60].

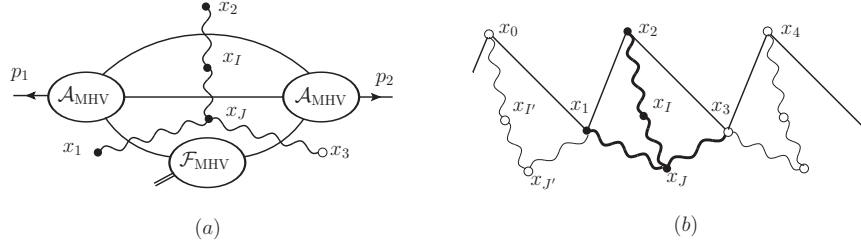


Figure 14: (a) First MHV diagram for a two-loop, two-point MHV form factor. (b) The corresponding dual MHV diagram.

$x_1 - x_3 = q$. Similarly, one can also introduce $x_{I'}$ such that $x_{I'} - x_I = q$. The dual MHV diagram is shown in Figure 15(b).

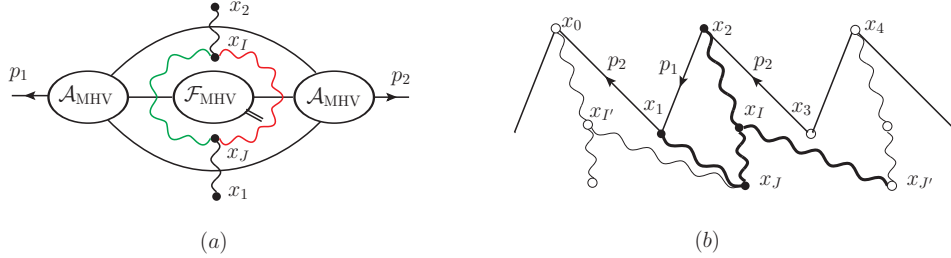


Figure 15: (a) Second MHV diagram for a two-loop, two-point MHV form factor. (b) The corresponding dual MHV diagram.

As before, we consider only translationally inequivalent diagrams within one period. Each such diagram will have two one-point external vertices, two three-point internal vertices and four propagators, as shown by dark bullets and dark wavy lines in Figure 15(b). The expression of this dual MHV diagram is then

$$\begin{aligned}
& \int d^4 x_I d^8 \Theta_I \frac{1}{\langle \ell_{I2} \ell_{IJ} \rangle \langle \ell_{IJ} \ell_{IJ'} \rangle \langle \ell_{IJ'} \ell_{I2} \rangle} \int d^4 x_J d^8 \Theta_J \frac{1}{\langle \ell_{J1} \ell_{JJ'} \rangle \langle \ell_{JJ'} \ell_{JI} \rangle \langle \ell_{JI} \ell_{J1} \rangle} \\
& \frac{\langle 12 \rangle}{\langle 1 \ell_{2I} \rangle \langle \ell_{2I} 2 \rangle} \frac{\langle 21 \rangle}{\langle 2 \ell_{1J} \rangle \langle \ell_{1J} 1 \rangle} \\
& \frac{1}{x_{I2}^2} \int d^4 \eta_{I2} \delta^{0|8}(\ell_{I2} \eta_{I2} + \Theta_{I2}) \frac{1}{x_{J1}^2} \int d^4 \eta_{J1} \delta^{0|8}(\ell_{J1} \eta_{J1} + \Theta_{J1}) \\
& \frac{1}{x_{IJ}^2} \int d^4 \eta_{IJ} \delta^{0|8}(\ell_{IJ} \eta_{IJ} + \Theta_{IJ}) \frac{1}{x_{IJ'}^2} \int d^4 \eta_{IJ'} \delta^{0|8}(\ell_{IJ'} \eta_{IJ'} + \Theta_{IJ'}) \\
& \int d^4 x_{I'} d^8 \Theta_{I'} \delta^4(x_{II'} + x_{13}) \delta^{0|8}(\Theta_{II'} + \Theta_{13}) \int d^4 x_{J'} d^8 \Theta_{J'} \delta^4(x_{JJ'} - x_{13}) \delta^{0|8}(\Theta_{JJ'} - \Theta_{13}) .
\end{aligned} \tag{5.9}$$

Notice in the last line of (5.9) the delta functions which enforce the periodicity of the super region momenta $x_{I'}$ and $x_{J'}$. One can check that (5.9) is indeed equivalent to the result of the conventional MHV diagram in Figure 15(a).

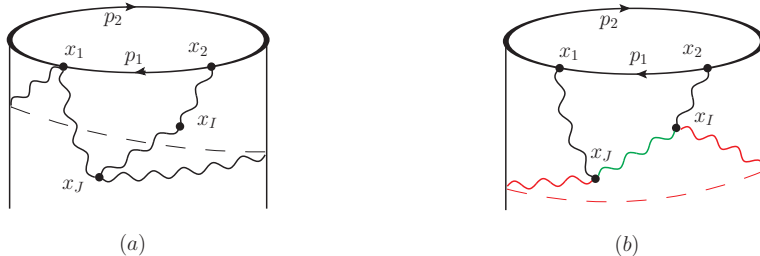


Figure 16: (a) Cylinder picture for the MHV diagram in Figure 14. (b) Cylinder picture for the MHV diagram in Figure 15. The period of the cylinder is q .

The dual MHV rules for form factors described above can be understood more naturally if we put the periodic configuration on a cylinder of period q , see Figure 16. In particular, Figure 16(b) corresponds to the MHV diagram in Figure 15. The two coloured propagators connecting x_I and x_J form a loop with winding momentum q , which exactly correspond to the coloured lines in the MHV diagram in Figure 15(a). We would like to stress a general feature of the rules we have described before, namely that no *single* propagator can stretch for one or more than one period around the cylinder.

The dual MHV rules can be applied to generic form factors. As in the case of amplitudes, in order to calculate an N^k MHV form factor at L loops, we need to sum over all allowed diagrams with

$$\#(\text{internal vertices}) = L, \quad \#(\text{propagators}) = k + 2L. \quad (5.10)$$

It would be very interesting to map the dual MHV rules described here to a dual Wilson line picture for form factors. We leave this question for future work.

Acknowledgements

It is a pleasure to thank Fernando Alday, Nima Arkani-Hamed, Mathew Bullimore, Bo Feng, Valeria Gili, Valya Khoze, Koji Hashimoto, Lionel Mason, Sri K. Pattabhi Jois, David Skinner, Wei Song, Bill Spence, Chung-I Tan, Alexander Zhiboedov, and especially Rutger Boels and Paul Heslop for sharing their insights. AB and GT would like to thank the KITP at the University of California, Santa Barbara, where their research was supported by the National Science Foundation under Grant No. NSF PHY05-51164, and Nima Arkani-Hamed for an invitation to the Institute for Advanced Study, Princeton, where some of the results of this paper were presented. GY would like to thank the hospitality of Hamburg University, Harvard University and Institute of Theoretical Physics, Chinese Academy of Sciences where part of this work

was done, and Paul Heslop for an invitation to the 11th Workshop on Non-Perturbative Quantum Chromodynamics, where the results of this paper were presented. This work was supported by the STFC under a Rolling Grant ST/G000565/1.

A Vanishing of form factors at large z

A.1 Bosonic form factors

In this appendix we consider a generic non-MHV bosonic form factor of the operator $\text{Tr}(\phi^2)$ and prove that, for a $[k, l]$ shift

$$\hat{\tilde{\lambda}}_k := \tilde{\lambda}_k + z\tilde{\lambda}_l, \quad \hat{\lambda}_l := \lambda_l - z\lambda_k, \quad (\text{A.1})$$

$F(z)$ vanishes as $z \rightarrow \infty$ if

$$(h_k, h_l) \text{ is equal to : } (0, +), (+, +), (-, +), (0, 0), (-, 0), (-, -). \quad (\text{A.2})$$

The proof is based on the MHV diagram expansion of form factors, and follows closely that for amplitudes presented in [23].

To begin with, it is immediate to see that an MHV form factor (2.3) with a $[k, l]$ shift vanishes as $z \rightarrow \infty$, with the only exception of the case $(h_k, h_l) = (+, 0)$. Consider now a generic non-MHV form factor. Each MHV diagram contributing to its expansion is a product of MHV vertices, times propagators $1/L^2$. These propagators will either be independent of z , or vanish when $z \rightarrow \infty$. As in [23], the spinors $\lambda_L = L[\tilde{\xi}]$ associated to internal legs can also be made z -independent by choosing the reference spinor $\tilde{\xi}$ to be equal to $\tilde{\xi} = \tilde{\lambda}_l$. Thus, dangerous z -dependent terms can only arise from terms affected by the shifts in the external legs k and l .

For the cases where (h_k, h_l) is $(\pm, +)$ or $(0, +)$, only the denominators acquire z -dependence, and hence $F(z)$ vanishes at large z . By using anti-MHV diagrams we arrive at the same result for the case where (h_k, h_l) is equal to either $(-, -)$ or $(-, 0)$. The case $(h_k, h_l) = (0, 0)$ needs special attention. The case when k and l belong to the same MHV vertex has already been considered, and leads to a falloff of the diagram as $z \rightarrow \infty$. When k and l belong to different vertices, there will be at least one propagator depending on z , which will provide a factor of $1/z$ at large z . The vertex involving leg l behaves asymptotically as z^2/z^2 regardless of whether it is an MHV form factor or a conventional MHV vertex, while all other vertices are independent of z . We conclude that each MHV diagram falls off as $1/z$ at large z .

We mention here that the argument described above can also be applied to scattering amplitudes. Shifting two scalars makes the amplitude vanish as $z \rightarrow \infty$ provided that the scalars take the same $SU(4)$ indices.

A.2 Supersymmetric form factors

As we have shown in the previous appendix, the bosonic form factor vanishes at infinity for an $[i, j]$ shift if i and j are both scalars. Here we want to use supersymmetry to relate the large- z behaviour of generic supersymmetric form factors to that of form factors with legs i and j being both scalars. This will then prove the validity of the supersymmetric BCFW recursion relation for all supersymmetric form factors in fashion similar to [53].

For supersymmetric non-chiral form factor $F(\lambda, \tilde{\lambda}, \eta_+, \tilde{\eta}^-)$, the $[i, j]$ shift is

$$\begin{aligned}\hat{\lambda}_i(z) &:= \tilde{\lambda}_i + z\tilde{\lambda}_j, & \hat{\lambda}_j &:= \lambda_j - z\lambda_i, \\ \hat{\eta}_{i,+} &:= \eta_{i,+} + z\eta_{j,+}, & \hat{\tilde{\eta}}_j^- &= \tilde{\eta}_j^- - z\tilde{\eta}_i^-. \end{aligned} \quad (\text{A.3})$$

As in [53], we choose a particular transformation where

$$\bar{Q}_{\tilde{\zeta}} = \tilde{\zeta}_{\dot{\alpha}+} \bar{Q}^{\dot{\alpha}+}, \quad Q_{\xi} = \xi_{\alpha}^- Q_{-}^{\alpha}, \quad (\text{A.4})$$

where

$$\tilde{\zeta} = \frac{1}{[i\ j]} \left(-\tilde{\lambda}_i \eta_j + \tilde{\lambda}_j \eta_i \right), \quad \xi = \frac{1}{\langle i\ j \rangle} \left(-\lambda_i \tilde{\eta}_j + \lambda_j \tilde{\eta}_i \right). \quad (\text{A.5})$$

One can check that their action on the fermionic coordinates $\eta_{k,+}, \tilde{\eta}_k^-$ is

$$e^{\bar{Q}_{\tilde{\zeta}}} \eta_{k,+} := \eta'_{k,+} = \eta_{k,+} - \eta_{i,+} \frac{[kj]}{[ij]} + \eta_{j,+} \frac{[ki]}{[ij]}, \quad (\text{A.6})$$

$$e^{Q_{\xi}} \tilde{\eta}_k^- := \tilde{\eta}'_k^- = \tilde{\eta}_k^- - \tilde{\eta}_i^- \frac{\langle kj \rangle}{\langle ij \rangle} + \tilde{\eta}_j^- \frac{\langle ki \rangle}{\langle ij \rangle}, \quad (\text{A.7})$$

and in particular $e^{\bar{Q}_{\tilde{\zeta}}} \eta_{i,+} = e^{\bar{Q}_{\tilde{\zeta}}} \eta_{j,+} = e^{Q_{\xi}} \tilde{\eta}_i^- = e^{Q_{\xi}} \tilde{\eta}_j^- = 0$. Since the form factor is invariant under \bar{Q}^+ and Q_- transformations, i.e. $e^{\bar{Q}_{\tilde{\zeta}}} \mathcal{F} = e^{Q_{\xi}} \mathcal{F} = \mathcal{F}$ (see (3.41)), we conclude that

$$\begin{aligned} & \mathcal{F}(\lambda_1, \tilde{\lambda}_1, \eta_{1,+}, \tilde{\eta}_1^-; \cdots; \lambda_i, \hat{\lambda}_i, \hat{\eta}_{i,+}, \hat{\tilde{\eta}}_i^-; \cdots; \hat{\lambda}_j, \tilde{\lambda}_j, \eta_{j,+}, \hat{\tilde{\eta}}_j^-; \cdots; \lambda_n, \tilde{\lambda}_n, \eta_{n,+}, \tilde{\eta}_n^-) \\ &= \mathcal{F}(\lambda_1, \tilde{\lambda}_1, \eta'_{1,+}, \tilde{\eta}'_1^-; \cdots; \lambda_i, \hat{\lambda}_i, 0, 0; \cdots; \hat{\lambda}_j, \tilde{\lambda}_j, 0, 0; \cdots; \lambda_n, \tilde{\lambda}_n, \eta'_{n,+}, \tilde{\eta}'_n^-). \end{aligned} \quad (\text{A.8})$$

Thus, we can always choose a supersymmetry transformation which sets i and j to be scalars. It is important to notice that under the $[i, j]$ shift, the transformed η'_+ and $\tilde{\eta}'_-$ variables are independent of z . The large- z behaviour of $\mathcal{F}(z)$ is therefore the same as that of the bosonic form factor with i and j being scalars. This case was considered in the previous appendix, and shown to fall off as $1/z$ at large z . Hence the statement is also true for the shifted supersymmetric form factor $\mathcal{F}(z)$. The proof illustrated above concerned the large- z behaviour of the full non-chiral super form factor, but a very similar one applies to the form factor in chiral superspace, since the latter is related to the former by a half-Fourier transform in superspace.


B Dual MHV rules

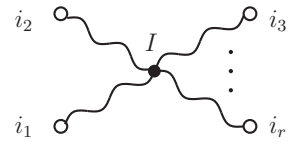
We recall that momenta and supermomenta for a massless particle are defined in terms of dual momenta and supermomenta as [57]

$$x_i - x_{i+1} = \lambda_i \tilde{\lambda}_i, \quad \Theta_i - \Theta_{i+1} = \lambda_i \eta_i, \quad (\text{B.1})$$

where $x_{ij} := x_i - x_j$ and $\Theta_{ij} := \Theta_i - \Theta_j$.

The dual MHV diagram rules of [56] are summarised in Figure 17.

(a)  $\frac{1}{x_{ij}^2} \int d^4 \eta_{ij} \delta^{0|8}(\ell_{ij} \eta_{ij} + \Theta_{ij})$

(b)  $g_{\text{YM}}^2 \int d^4 x_I d^8 \Theta_I \frac{1}{\langle \ell_{I1} \ell_{I2} \rangle \langle \ell_{I2} \ell_{I3} \rangle \cdots \langle \ell_{Ir-1} \ell_{Ir} \rangle \langle \ell_{Ir} \ell_{I1} \rangle}$

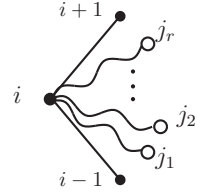
(c)  $\frac{\langle i-1 \ i \rangle}{\langle i-1 \ \ell_{ij1} \rangle \langle \ell_{ij1} \ell_{ij2} \rangle \langle \ell_{ij2} \ell_{ij3} \rangle \cdots \langle \ell_{ijr-1} \ell_{ijr} \rangle \langle \ell_{ijr} \ i \rangle}$

Figure 17: *Feynman rules for dual MHV diagrams. (a) Propagator. (b) r-point internal vertex. (c) r-point external vertex.*

In these rules, the off-shell continuation for spinors associated to internal legs, $|\ell_{ij}\rangle$, is defined as usual as [21]

$$|\ell_{ij}\rangle := x_{ij}|\xi], \quad (\text{B.2})$$

where $|\xi]$ is an arbitrary reference spinor.

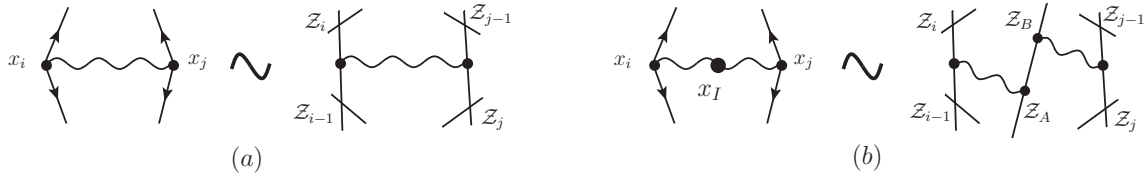


Figure 18: *Dual MHV diagrams for (a) a NMHV tree amplitude, and (b) a one-loop MHV amplitude, and the corresponding momentum twistor diagrams.*

For convenience, we recall here two simple applications of these rules from [56]. A generic dual MHV diagram contributing to an NMHV tree amplitude is pictured

in Figure 18(a). There are two boundary vertices and one propagator. By applying the dual MHV rules of Figure 17, we get

$$\frac{\langle i-1 \ i \rangle}{\langle i-1 \ \ell_{ij} \rangle \langle \ell_{ij} \ i \rangle} \frac{\langle j-1 \ j \rangle}{\langle j-1 \ \ell_{ij} \rangle \langle \ell_{ij} \ j \rangle} \frac{1}{x_{ij}^2} \int d^4 \eta_{ij} \delta^{0|8}(\ell_{ij} \eta_{ij} + \Theta_{ij}) , \quad (\text{B.3})$$

which can be easily translated in terms of the superconformal invariant R -function $R_{*,ij} := [* , i-1, i, j-1, j]$, with

$$[i, j, k, l, m] \equiv \frac{\delta^{(4)}(\langle i \ j \ k \ l \rangle \chi_m + \text{cyclic terms})}{\langle i \ j \ k \ l \rangle \langle j \ k \ l \ m \rangle \langle k \ l \ m \ i \rangle \langle l \ m \ i \ j \rangle \langle m \ i \ j \ k \rangle} . \quad (\text{B.4})$$

The reference momentum twistor is $\mathcal{Z}_* = (0, \xi, 0)$.

Similarly, a generic dual MHV diagram for a one-loop MHV amplitude is depicted in Figure 18(b) and is equal to

$$g_{\text{YM}}^2 \int d^4 x_I d^8 \Theta_I \frac{1}{\langle \ell_{iI} \ell_{Ij} \rangle \langle \ell_{Ij} \ell_{iI} \rangle} \frac{\langle i-1 \ i \rangle}{\langle i-1 \ \ell_{iI} \rangle \langle \ell_{iI} \ i \rangle} \frac{\langle j-1 \ j \rangle}{\langle j-1 \ \ell_{Ij} \rangle \langle \ell_{Ij} \ j \rangle} \frac{1}{x_{iI}^2} \int d^4 \eta_{iI} \delta^{0|8}(\ell_{iI} \eta_{iI} + \Theta_{iI}) \frac{1}{x_{Ij}^2} \int d^4 \eta_{Ij} \delta^{0|8}(\ell_{Ij} \eta_{Ij} + \Theta_{Ij}) . \quad (\text{B.5})$$

In terms of momentum twistor variables this becomes [55],

$$g_{\text{YM}}^2 \int d^{3|4} \mathcal{Z}_A \wedge d^{3|4} \mathcal{Z}_B \ [*, i-1, i, A, B'] [*, j-1, j, A, B''] , \quad (\text{B.6})$$

where $(x_I, \Theta_I) \sim \mathcal{Z}_A \wedge \mathcal{Z}_B$ and

$$B' = (A, B) \cap (*, j-1, j) , \quad B'' = (A, B) \cap (*, i-1, i) . \quad (\text{B.7})$$

References

- [1] A. H. Mueller, *On The Asymptotic Behavior Of The Sudakov Form-Factor*, Phys. Rev. D **20** (1979) 2037.
- [2] J. C. Collins, *Algorithm To Compute Corrections To The Sudakov Form-Factor*, Phys. Rev. D **22** (1980) 1478.
- [3] A. Sen, *Asymptotic Behavior Of The Sudakov Form-Factor In QCD*, Phys. Rev. D **24** (1981) 3281.

- [4] S. Catani and L. Trentadue, *Resummation Of The QCD Perturbative Series For Hard Processes*, Nucl. Phys. B **327** (1989) 323.
- [5] L. Magnea and G. Sterman, *Analytic continuation of the Sudakov form-factor in QCD*, Phys. Rev. D **42** (1990) 4222.
- [6] S. Catani, *The singular behaviour of QCD amplitudes at two-loop order*, Phys. Lett. B **427** (1998) 161 [arXiv:hep-ph/9802439].
- [7] G. Sterman and M. E. Tejeda-Yeomans, *Multi-loop amplitudes and resummation*, Phys. Lett. B **552** (2003) 48 [arXiv:hep-ph/0210130].
- [8] G. P. Korchemsky, A. V. Radyushkin, *Loop Space Formalism And Renormalization Group For The Infrared Asymptotics Of Qcd*, Phys. Lett. **B171** (1986) 459-467.
- [9] G. P. Korchemsky, *Asymptotics of the Altarelli-Parisi-Lipatov Evolution Kernels of Parton Distributions*, Mod. Phys. Lett. **A4** (1989) 1257-1276.
- [10] Z. Bern, L. J. Dixon and V. A. Smirnov, *Iteration of planar amplitudes in maximally supersymmetric Yang-Mills theory at three loops and beyond*, Phys. Rev. D **72** (2005) 085001 [arXiv:hep-th/0505205].
- [11] L. F. Alday, D. Gaiotto, J. Maldacena, A. Sever and P. Vieira, *An Operator Product Expansion for Polygonal null Wilson Loops*, JHEP **1104**, 088 (2011) [arXiv:1006.2788 [hep-th]].
- [12] N. Beisert, C. Ahn, L. F. Alday, Z. Bajnok, J. M. Drummond, L. Freyhult, N. Gromov, R. A. Janik *et al.*, *Review of AdS/CFT Integrability: An Overview*, [arXiv:1012.3982 [hep-th]].
- [13] L. F. Alday, D. Gaiotto, J. Maldacena, *Thermodynamic Bubble Ansatz*, [arXiv:0911.4708 [hep-th]].
- [14] L. F. Alday, J. Maldacena, A. Sever, P. Vieira, *Y-system for Scattering Amplitudes*, J. Phys. A **A43** (2010) 485401. [arXiv:1002.2459 [hep-th]].
- [15] L. F. Alday and J. Maldacena, *Comments on gluon scattering amplitudes via AdS/CFT*, JHEP **0711** (2007) 068 [arXiv:0710.1060 [hep-th]].
- [16] J. Maldacena and A. Zhiboedov, *Form factors at strong coupling via a Y-system*, JHEP **1011**, 104 (2010) [arXiv:1009.1139 [hep-th]].
- [17] W. L. van Neerven, *Infrared Behavior Of On-Shell Form-Factors In A N=4 Supersymmetric Yang-Mills Field Theory*, Z. Phys. C **30** (1986) 595.

- [18] A. Brandhuber, B. Spence, G. Travaglini and G. Yang, *Form Factors in $N=4$ Super Yang-Mills and Periodic Wilson Loops*, JHEP **1101** (2011) 134 [[arXiv:1011.1899 \[hep-th\]](#)].
- [19] L. V. Bork, D. I. Kazakov and G. S. Vartanov, *On form factors in $N=4$ SYM*, JHEP **1102** (2011) 063 [[arXiv:1011.2440 \[hep-th\]](#)].
- [20] M. L. Mangano, S. J. Parke, Z. Xu, *Duality and Multi - Gluon Scattering*, Nucl. Phys. **B298** (1988) 653.
- [21] F. Cachazo, P. Svrcek and E. Witten, *MHV vertices and tree amplitudes in gauge theory*, JHEP **0409** (2004) 006 [[arXiv:hep-th/0403047](#)].
- [22] R. Britto, F. Cachazo and B. Feng, *New Recursion Relations for Tree Amplitudes of Gluons*, Nucl. Phys. B **715** (2005) 499 [[arXiv:hep-th/0412308](#)].
- [23] R. Britto, F. Cachazo, B. Feng and E. Witten, *Direct Proof Of Tree-Level Recursion Relation In Yang-Mills Theory*, Phys. Rev. Lett. **94** (2005) 181602 [[arXiv:hep-th/0501052](#)].
- [24] P. Mansfield, *The Lagrangian origin of MHV rules*, JHEP **0603** (2006) 037 [[hep-th/0511264](#)].
- [25] S. Weinberg, *The Quantum theory of fields. Vol. 1: Foundations*, Cambridge University Press, 1995.
- [26] R. Britto, B. Feng, R. Roiban, M. Spradlin, A. Volovich, *All split helicity tree-level gluon amplitudes*, Phys. Rev. **D71** (2005) 105017 [[hep-th/0503198](#)].
- [27] A. Galperin, E. Ivanov, S. Kalitsyn, V. Ogievetsky, E. Sokatchev, *Unconstrained $N=2$ Matter, Yang-Mills and Supergravity Theories in Harmonic Superspace*, Class. Quant. Grav. **1** (1984) 469-498.
- [28] A. Galperin, E. Ivanov, V. Ogievetsky and E. Sokatchev, *Harmonic Superspace*, Cambridge University Press (2001).
- [29] B. Eden, P. Heslop, G. P. Korchemsky and E. Sokatchev, *The super-correlator/super-amplitude duality: Part I*, [arXiv:1103.3714 \[hep-th\]](#).
- [30] B. Eden, P. Heslop, G. P. Korchemsky and E. Sokatchev, *The super-correlator/super-amplitude duality: Part II*, [arXiv:1103.4353 \[hep-th\]](#).
- [31] V. P. Nair, *A current algebra for some gauge theory amplitudes*, Phys. Lett. B **214** (1988) 215.
- [32] L. F. Alday and J. Maldacena, *Gluon scattering amplitudes at strong coupling*, JHEP **0706** (2007) 064 [[arXiv:0705.0303 \[hep-th\]](#)].

- [33] J. M. Drummond, G. P. Korchemsky and E. Sokatchev, *Conformal properties of four-gluon planar amplitudes and Wilson loops*, Nucl. Phys. B **795** (2008) 385 [[arXiv:0707.0243](#) [[hep-th](#)]].
- [34] A. Brandhuber, P. Heslop and G. Travaglini, *MHV Amplitudes in $N=4$ Super Yang-Mills and Wilson Loops*, Nucl. Phys. B **794** (2008) 231 [[arXiv:0707.1153](#) [[hep-th](#)]].
- [35] A. Brandhuber, B. Spence and G. Travaglini, *Tree-Level Formalism*, to appear in J. Phys. A, [arXiv:1103.3477](#) [[hep-th](#)].
- [36] A. Brandhuber, B. Spence and G. Travaglini, *One-loop gauge theory amplitudes in $N=4$ super Yang-Mills from MHV vertices*, Nucl. Phys. B **706** (2005) 150 [[arXiv:hep-th/0407214](#)].
- [37] E. Witten, *Perturbative gauge theory as a string theory in twistor space*, Commun. Math. Phys. **252** (2004) 189 [[arXiv:hep-th/0312171](#)].
- [38] M. T. Grisaru, H. N. Pendleton and P. van Nieuwenhuizen, *Supergravity and the S Matrix*, Phys. Rev. D **15** (1977) 996.
- [39] M. T. Grisaru and H. N. Pendleton, *Some Properties of Scattering Amplitudes in Supersymmetric Theories*, Nucl. Phys. B **124** (1977) 81.
- [40] M. L. Mangano and S. J. Parke, *Multiparton amplitudes in gauge theories*, Phys. Rept. **200** (1991) 301 [[arXiv:hep-th/0509223](#)].
- [41] H. Elvang, D. Z. Freedman, M. Kiermaier, *SUSY Ward identities, Superamplitudes, and Counterterms* [[arXiv:1012.3401](#) [[hep-th](#)]].
- [42] K. A. Intriligator, *Bonus symmetries of $N=4$ superYang-Mills correlation functions via AdS duality*, Nucl. Phys. **B551** (1999) 575-600 [[hep-th/9811047](#)].
- [43] B. Eden, P. S. Howe, C. Schubert, E. Sokatchev, P. C. West, *Extremal correlators in four-dimensional SCFT*, Phys. Lett. **B472** (2000) 323-331 [[hep-th/9910150](#)].
- [44] B. Eden, C. Schubert, E. Sokatchev, *Three loop four point correlator in $N=4$ SYM*, Phys. Lett. **B482** (2000) 309-314 [[hep-th/0003096](#)].
- [45] L. J. Dixon, E. W. N. Glover and V. V. Khoze, *MHV rules for Higgs plus multi-gluon amplitudes*, JHEP **0412** (2004) 015 [[arXiv:hep-th/0411092](#)].
- [46] Y. -t. Huang, *Non-Chiral S-Matrix of $N=4$ Super Yang-Mills* [[arXiv:1104.2021](#) [[hep-th](#)]].

- [47] Z. Bern, L. J. Dixon, D. C. Dunbar and D. A. Kosower, *One Loop N Point Gauge Theory Amplitudes, Unitarity And Collinear Limits*, Nucl. Phys. B **425** (1994) 217 [arXiv:hep-ph/9403226].
- [48] Z. Bern, L. J. Dixon, D. C. Dunbar and D. A. Kosower, *Fusing gauge theory tree amplitudes into loop amplitudes*, Nucl. Phys. B **435**, 59 (1995) [arXiv:hep-ph/9409265].
- [49] Z. Bern, L. J. Dixon, D. A. Kosower, *Two-loop $g \rightarrow g$ gg splitting amplitudes in QCD*, JHEP **0408** (2004) 012 [hep-ph/0404293].
- [50] R. Britto, F. Cachazo, B. Feng, *Generalized unitarity and one-loop amplitudes in $N=4$ super-Yang-Mills*, Nucl. Phys. **B725** (2005) 275-305 [hep-th/0412103].
- [51] H. Elvang, D. Z. Freedman, M. Kiermaier, *Proof of the MHV vertex expansion for all tree amplitudes in $N=4$ SYM theory*, JHEP **0906**, 068 (2009) [arXiv:0811.3624 [hep-th]].
- [52] A. Brandhuber, P. Heslop, G. Travaglini, *A Note on dual superconformal symmetry of the $N=4$ super Yang-Mills S-matrix*, Phys. Rev. **D78** (2008) 125005 [arXiv:0807.4097 [hep-th]].
- [53] N. Arkani-Hamed, F. Cachazo, J. Kaplan, *What is the Simplest Quantum Field Theory?*, JHEP **1009** (2010) 016 [arXiv:0808.1446 [hep-th]].
- [54] L. J. Mason, D. Skinner, *The Complete Planar S-matrix of $N=4$ SYM as a Wilson Loop in Twistor Space*, JHEP **1012** (2010) 018 [arXiv:1009.2225 [hep-th]].
- [55] M. Bullimore, L. J. Mason, D. Skinner, *MHV Diagrams in Momentum Twistor Space*, JHEP **1012** (2010) 032 [arXiv:1009.1854 [hep-th]].
- [56] A. Brandhuber, B. Spence, G. Travaglini, G. Yang, *A Note on Dual MHV Diagrams in $N=4$ SYM*, JHEP **1012** (2010) 087 [arXiv:1010.1498 [hep-th]].
- [57] J. M. Drummond, J. Henn, G. P. Korchemsky, E. Sokatchev, *Dual superconformal symmetry of scattering amplitudes in $N=4$ super-Yang-Mills theory*, Nucl. Phys. **B828** (2010) 317-374 [arXiv:0807.1095 [hep-th]].
- [58] A. Hodges, *Eliminating spurious poles from gauge-theoretic amplitudes* [arXiv:0905.1473 [hep-th]].
- [59] A. Brandhuber, B. Spence, G. Travaglini, *From trees to loops and back*, JHEP **0601** (2006) 142 [hep-th/0510253].
- [60] N. Arkani-Hamed, J. L. Bourjaily, F. Cachazo, S. Caron-Huot, J. Trnka, *The All-Loop Integrand For Scattering Amplitudes in Planar $N=4$ SYM*, JHEP **1101** (2011) 041 [arXiv:1008.2958 [hep-th]].